Physical Science International Journal

22(1): 1-44, 2019; Article no.PSIJ.48372
ISSN: 2348-0130

Plasmas Computed with ATMED CR of the 3rd Non-LTE Code Comparison Workshop Database

A. J. Benita[1,2*]

[1]Plasma Atomic Physics Group, Madrid Polytechnic University, 28006, Madrid, Spain.
[2]Department of Physics, Las Palmas Canary Islands University, 35017, Las Palmas de Gran Canaria, Spain.

Author's contribution

The sole author designed, analysed, interpreted and prepared the manuscript.

Article Information

DOI: 10.9734/PSIJ/2019/v22i130122
Editor(s):
(1) Dr. Rami Ahmad El-Nabulsi, Athens Institute for Education and Research, Mathematics and Physics Divisions, Greece.
(2) Dr. Christian Brosseau, Distinguished Professor, Department of Physics, Université de Bretagne Occidentale, France.
Reviewers:
(1) A. Ayeshamariam, Khadir Mohideen College, India.
(2) Francisco Bulnes, Tecnológico de Estudios Superiores de Chalco, Mexico.
(3) Abdullah Sonmezoglu, Bozok University,Turkey.
(4) Orchidea Maria Lecian, Sapienza University of Rome, Italy.
(5) Pasupuleti Venkata Siva Kumar, Vallurupalli Nageswara Rao Vignana Jyothi Institute of Engineering &Technology, India.
Complete Peer review History: http://www.sdiarticle3.com/review-history/48372

Original Research Article

Received 29 January 2019
Accepted 12 April 2019
Published 23 April 2019

ABSTRACT

In this paper, there are presented some results calculated with ATMED CR of the 3rd Non-LTE Code Comparison Workshop held in December 2003, when this software didn't exist, having been released in 2017. NLTE population kinetics codes were tested of steady-state cases for C, Al, Ar, Ge, Xe and Au plasmas selected for detailed comparisons. The scope of the meeting consisted of analyzing steady-state dense plasma cases of carbon, low temperature plasmas of aluminium and argon, X-ray laser experiments of germanium also with imposing a Planckian radiation field, medium- and high-Z multicharged ions of hot "experiment-related" plasmas of xenon, using real electron temperature and density parameters inferred from electronic and ionic Thomson scattering spectra and finally plasmas of gold. Being motivated by germanium X-ray laser experiments, the time history of electronic temperature T_e and density N_e for a temporal dependent case is provided in Workshop NLTE-3. The calculation with ATMED CR has been carried out to t = 1.975 ns considering the non-uniform time grid along with the corresponding values of T_e and N_e presented, being the initial condition LTE at low temperature.

**Corresponding author: E-mail: anajosefa.benita@upm.es, anajosefa.benita.cerdan@alumnos.upm.es;*

The results for plasma properties can be considered as relatively precise and optimal, being checked fundamentally the high sensitivity of calculations to changes in regime, local thermodynamic equilibrium (LTE) or non-LTE (NLTE), electronic and radiation temperatures, electronic density and the percentage of hot electrons. Frequency resolved and mean opacities are also displayed computed with ATMED CR using UTA (Unresolved Transition Array) or Mixed UTA formalisms.

Keywords: Screened hydrogenic atomic model; collisional radiative average atom code; plasmas of NLTE-3 workshop.

1. INTRODUCTION

The collisional radiative model ATMED CR [1,2] constructed in the Average Atom formalism has been developed to calculate plasma population kinetics under coronal, local or non-local thermodynamic equilibrium regimes as an extension of the module named ATMED LTE [3-5] designed previously for local thermodynamic conditions. The atomic model is based on a New Relativistic Screened Hydrogenic Model (NRSHM) with a set of universal screening constants including *nlj*-splitting that has been obtained by fitting to a large database of 61,350 atomic high quality data entries, compiled from the National Institute of Standards and Technology (NIST) database of U.S. Department of Commerce and from the Flexible Atomic Code (FAC) [6,7].

The calculation of accurate relativistic atomic populations including *nlj*-splitting of electronic orbitals, improves the precision of atomic properties as mean charge, rates and the resolution of spectral properties as opacities and radiative power losses, with respect to collisional radiative (CR) average atom codes as XSN of W. Lokke and W. Grasberger of 1977 with *n*-splitting [8,9] or considering nl-splitting [10-13]. The CR balance is based on iterative loops for reaching auto convergence in populations and plasma mean charge following the procedure of A.F. Nikiforov et al. [14]. The accuracy ATMED CR code can achieve can be consulted in Section 3 of Ref. [15] which explains in detail the phases of the investigation project, consisting of the comparison of plasma properties of this software with bibliographic data.

The implementation of the collisional radiative balance with the new atomic model, allows now to compute plasmas in NLTE regime or coronal regime, widening considerably for all chemical elements the validity range of thermodynamic conditions [16,17]. In Section 2 there are modeled plasmas with ATMED CR illustrating the high agreement with results for plasma properties of other codes participants of Workshop NLTE-3. Section 3 contains main conclusions. Details about the workshop, motivations for the chosen cases and discussion of some representative results can be found in References [18-19].

2. PLASMAS OF 3RD NLTE DATABASE

The following problems proposed for the cases of C, Al, Ar, Ge, Xe and Au atoms have been calculated with the collisional radiative average atom code ATMED CR. Some graphs are displayed by courtesy of the database (https://nlte.nist.gov/SAHA) for visual comparison of plasma properties. The indicated range of mean charge for NLTE-3 database is approximated. The Radiative Power Losses are indicated in (1e-7 x J)/cm^3/s ≡ erg/cm^3/s.

2.1 Carbon Plasmas

The following problems have been established for the steady-state cases of carbon atoms on a grid of electron temperatures and electron densities, see Table 1 and Fig. 1:

Element	Case ID	Total # of Points	Parameter	Grid	# of Points
Carbon	C	7	T_e	10, 15, 20, 30, 45, 60, 80	7
			N_e	10^{22}	1

Table 1. Carbon plasma properties of ATMED CR for comparison with codes of NLTE-3 workshop

N_e (cm^{-3}) = 10^{22}	ρ (g/cm^3)	Z_{bar} ATMED	Z_{bar} NLTE-3	η_e ATMED CR	RPL (1e-7 $J/cm^3/s$)
T_e = 10 eV	1.138E-01	1.753E+00	0.5÷2	-2.9307E+00	5.343969E+24
T_e = 15 eV	7.680E-02	2.598E+00	1.25÷2.8	-3.5470E+00	2.052203E+24
T_e = 20 eV	6.250E-02	3.195E+00	1.8÷3.4	-3.9812E+00	1.223476E+24
T_e = 30 eV	5.276E-02	3.781E+00	2.5÷3.8	-4.5934E+00	6.349924E+23
T_e = 45 eV	4.914E-02	4.059E+00	3÷4	-5.2034E+00	3.546953E+23
T_e = 60 eV	4.528E-02	4.404E+00	3.5÷4.5	-5.6356E+00	2.219607E+23
T_e = 80 eV	3.935E-02	5.068E+00	4.4÷5.1	-6.0676E+00	1.348140E+23

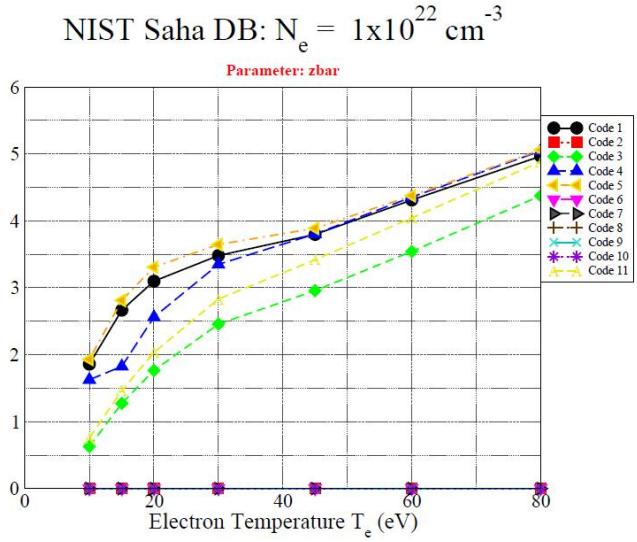

Fig. 1.a. Carbon plasma mean charge computed with codes of NLTE-3 workshop

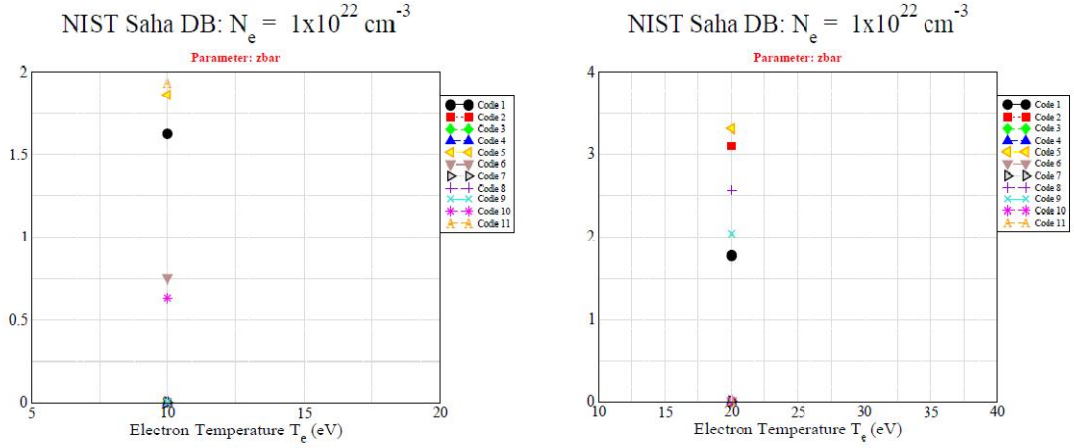

Fig. 1.b. Carbon plasma mean charge of density-temperature points computed with codes of NLTE-3 workshop

AT

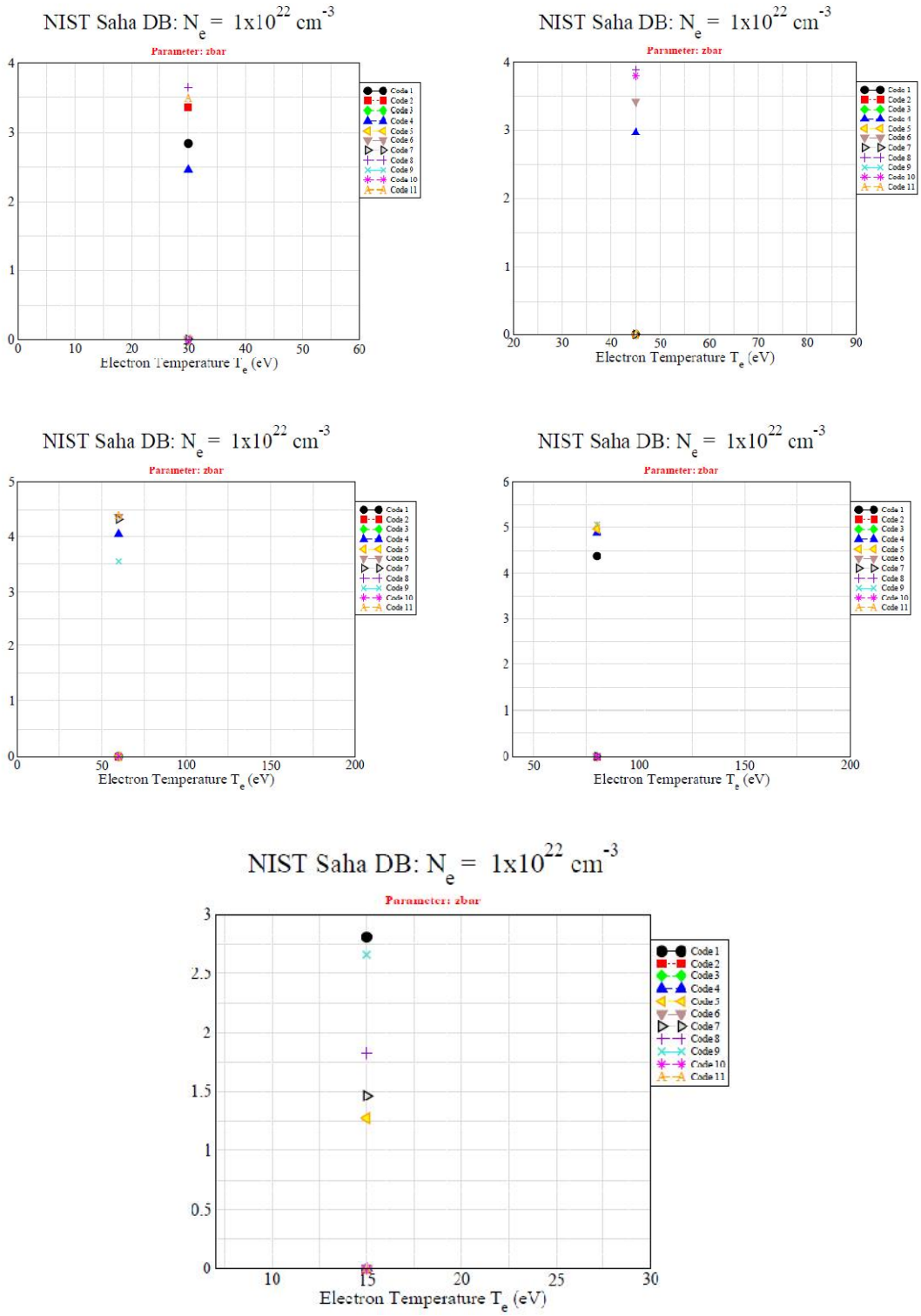

Fig. 1.b. Carbon plasma mean charge of density-temperature points computed with codes of NLTE-3 workshop

2.2 Aluminium Plasmas

The following problems have been established for the steady-state cases of aluminium atoms on a grid of electron temperatures and electron densities, see Table 2 and Fig. 2:

Element	Case ID	Total # of Points	Parameter	Grid	# of Points
Aluminum	Al	14	T_e	50, 70, 100, 150, 200, 400, 800	7
			N_e	10^{20}, 10^{22}	2

Table 2. Aluminium plasma properties of ATMED CR for comparison with codes of NLTE-3 workshop

N_e (cm^{-3}) = 10^{20}	ρ (g/cm^3)	Z_{bar} ATMED	Z_{bar} NLTE-3	η_e ATMED CR	RPL (1e-7 $J/cm^3/s$)
T_e = 50 eV	5.680E-04	7.933E+00	7.75÷9	-9.9628E+00	3.686132E+18
T_e = 70 eV	5.060E-04	8.866E+00	9.5÷10.5	-1.0472E+01	3.889779E+18
T_e = 100 eV	4.513E-04	9.929E+00	10.5÷11	-1.1008E+01	2.996605E+18
T_e = 150 eV	4.211E-04	1.064E+01	10.5÷11.5	-1.1616E+01	1.683416E+18
T_e = 200 eV	4.131E-04	1.085E+01	10.5÷11.5	-1.2048E+01	1.126856E+18
T_e = 400 eV	4.094E-04	1.094E+01	11÷11.5	-1.3088E+01	1.063361E+18
T_e = 800 eV	4.092E-04	1.095E+01	11÷12.5	-1.4127E+01	2.089232E+18
N_e (cm^{-3}) = 10^{22}	ρ (g/cm^3)	Z_{bar} ATMED	Zbar NLTE-3	η_e ATMED CR	RPL (1e-7 $J/cm^3/s$)
T_e = 50 eV	6.357E-02	7.053E+00	5.5÷7.5	-5.3610E+00	4.246858E+23
T_e = 70 eV	5.106E-02	8.781E+00	7.5÷9	-5.8663E+00	2.138201E+23
T_e = 100 eV	4.380E-02	1.023E+01	9.5÷10.5	-6.4022E+00	1.089358E+23
T_e = 150 eV	4.123E-02	1.087E+01	10÷11	-7.0109E+00	6.186111E+22
T_e = 200 eV	4.081E-02	1.098E+01	10.5÷11.5	-7.4426E+00	3.218611E+22
T_e = 400 eV	4.026E-02	1.113E+01	11÷12	-8.4824E+00	4.849790E+22
T_e = 800 eV	3.894E-02	1.151E+01	12.5	-9.5222E+00	6.303487E+22

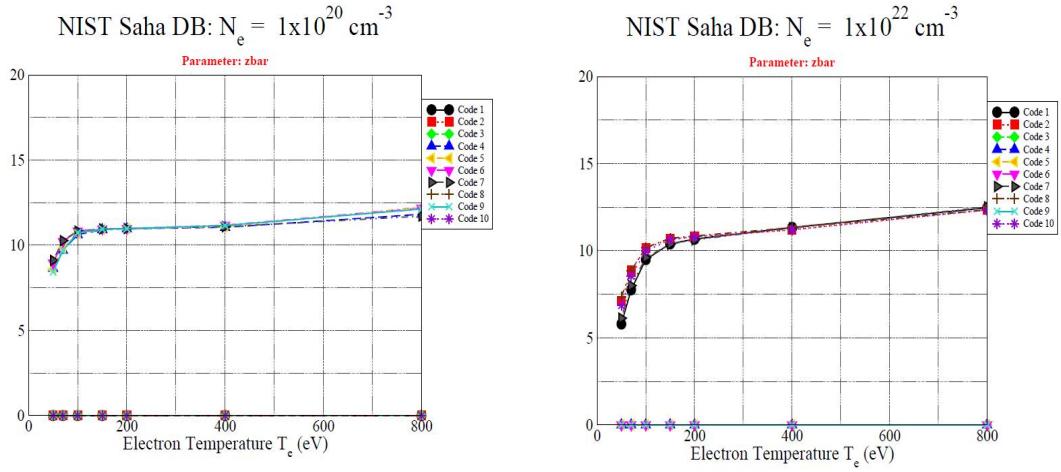

Fig. 2.a. Aluminium plasma mean charge computed with codes of NLTE-3 workshop

AT

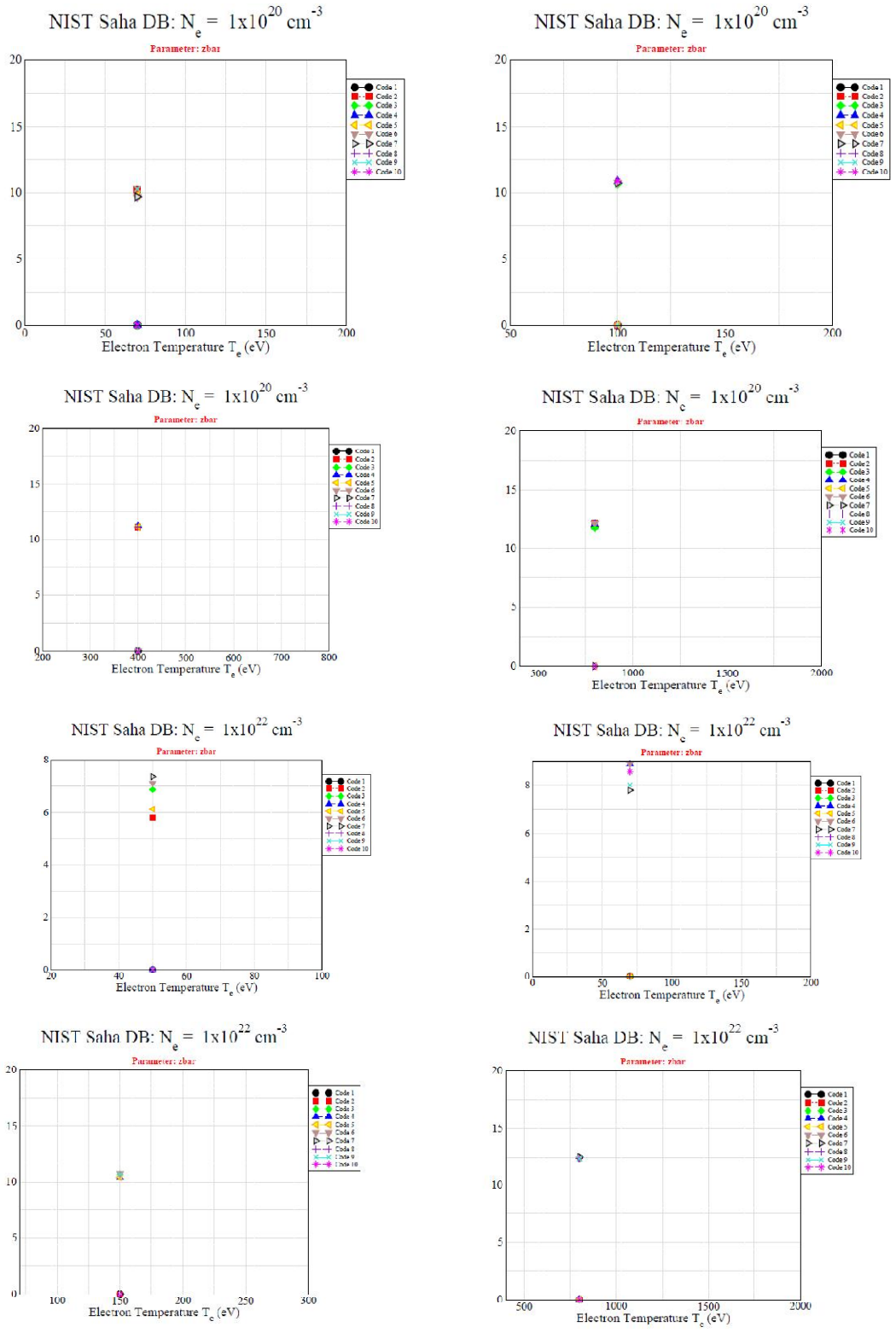

Fig. 2.b. Aluminium plasma mean charge of density-temperature points computed with codes of NLTE-3 workshop

2.3 Argon Plasmas

The following problems have been established for the steady-state cases of argon atoms on a grid of electron temperatures and electron densities, see Table 3 and Fig. 3:

Element	Case ID	Total # of Points	Parameter	Grid	# of Points
Argon	Ar	24	T_e	100, 300, 600, 1000	4
			N_e	10^{12}, 10^{18}, 10^{23}	3
			T_{hot}	10 000 eV at 0% and 10% of N_e	2

As a general remark, all trends of parameters must be carefully examined for each element and for a wide range of densities, temperatures and fractions and temperatures of hot electrons.

2.3.1 T_{hot} = 10000 eV at 0% of N_e

It is indicated the splitting of the bound-free oscillator strength for the case of low density 10^{12} cm^{-3}.

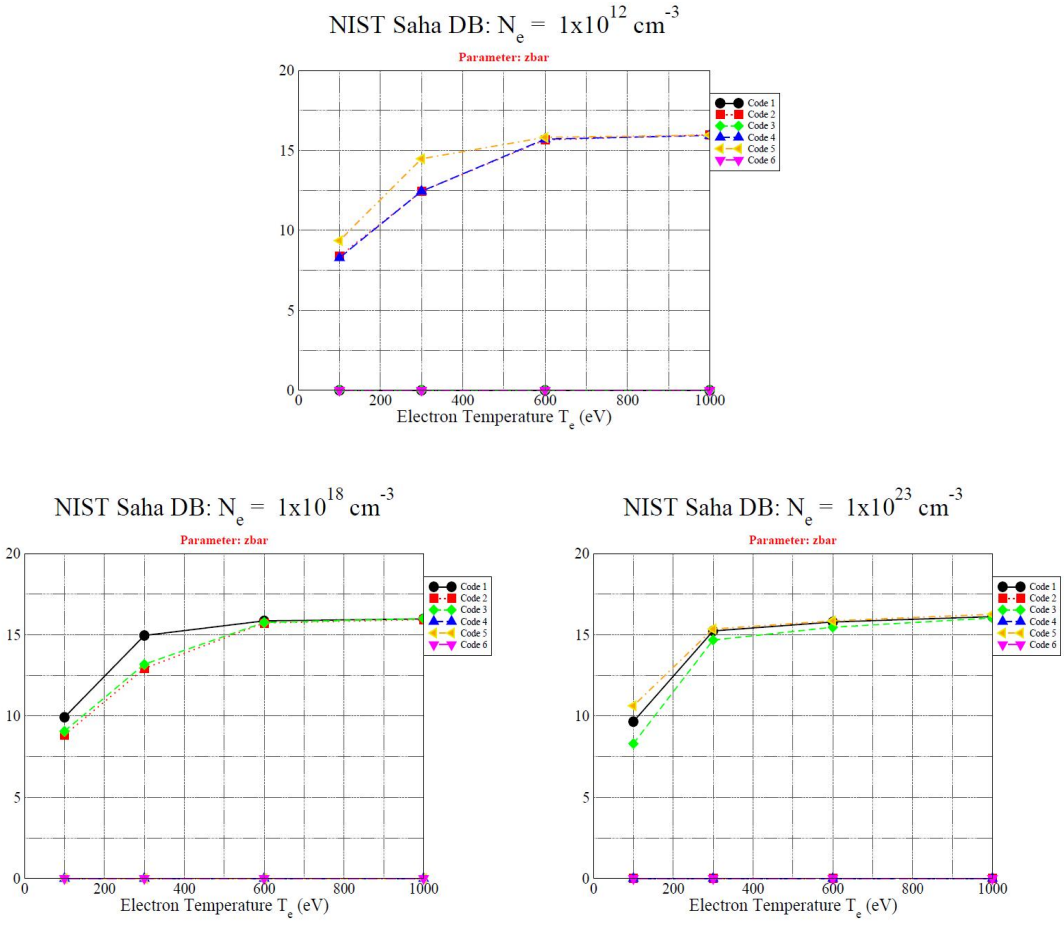

Fig. 3.a. Argon plasma mean charge computed with codes of NLTE-3 workshop

AT

Table 3.a. Argon plasma properties of ATMED CR for comparison with codes of NLTE-3 workshop

n-splitting & N_e (cm^{-3})=10^{12}	ρ (g/cm^3)	Z_{bar} ATMED	Z_{bar} NLTE-3	η_e ATMED CR	RPL (1e-7 $J/cm^3/s$)
T_e = 100 eV	8.340E-12	8.016E+00	8.5÷10	-2.9421E+01	1.497296E+06
T_e = 300 eV	8.340E-12	8.025E+00	12.5÷15	-3.1068E+01	4.314711E+06
nl-splitting & N_e (cm^{-3})=10^{12}	ρ (g/cm^3)	Z_{bar} ATMED	Z_{bar} NLTE-3	η_e ATMED CR	RPL (1e-7 $J/cm^3/s$)
T_e = 100 eV	8.340E-12	7.999E+00	8.5÷10	-2.9423E+01	2.445724E+04
T_e = 300 eV	8.300E-12	8.017E+00	12.5÷15	-3.1074E+01	1.170868E+05
N_e (cm^{-3}) = 10^{18}	ρ (g/cm^3)	Z_{bar} ATMED	Z_{bar} NLTE-3	η_e ATMED CR	RPL (1e-7 $J/cm^3/s$)
T_e = 100 eV	6.948E-06	9.548E+00	8.5÷10	-1.5613E+01	1.240592E+15
T_e = 300 eV	5.616E-06	1.181E+01	12.5÷15	-1.7261E+01	7.847624E+15
T_e = 600 eV	5.500E-06	1.294E+01	15.7÷16	-1.8231E+01	1.973927E+16
T_e = 1000 eV	5.400E-06	1.322E+01	16	-1.8994E+01	3.158257E+16
N_e (cm^{-3}) = 10^{23}	ρ (g/cm^3)	Z_{bar} ATMED	Z_{bar} NLTE-3	η_e ATMED CR	RPL (1e-7 $J/cm^3/s$)
T_e = 100 eV	1.120E+00	5.927E+00	8÷11	-4.0939E+00	2.499256E+27
T_e = 300 eV	4.580E-01	1.458E+01	14.5÷15.5	-5.7405E+00	8.180175E+25
T_e = 600 eV	4.220E-01	1.577E+01	15÷16	-6.7843E+00	3.201595E+25
T_e = 1000 eV	4.000E-01	1.660E+01	16÷17	-7.5532E+00	2.125694E+25

Table 3.b. Argon plasma properties of ATMED CR of NLTE-3 workshop

N_e (cm^{-3}) = 10^{18}	Z_{bar} WO hot	Z_{bar} W hot	η_e ATMED CR	ρ W hot (g/cm^3)	ρ WO hot (g/cm^3)	% Hot electrons
T_e = 100 eV	9.548E+00	9.614E+00	-1.5606E+01	6.948E-06	6.948E-06	**10%**
T_e = 100 eV	9.548E+00	1.018E+01	-1.5585E+01	6.700E-06	6.948E-06	**50%**
T_e = 300 eV	1.181E+01	1.187E+01	-1.7257E+01	5.616E-06	5.616E-06	**10%**
T_e = 300 eV	1.181E+01	1.800E+01	-1.7231E+01	3.800E-06	5.616E-06	**50%**
T_e = 600 eV	1.294E+01	1.292E+01	-1.8270E+01	5.300E-06	5.500E-06	**10%**
T_e = 600 eV	1.294E+01	1.301E+01	-1.8282E+01	5.200E-06	5.500E-06	**50%**
T_e = 1000 eV	1.322E+01	1.324E+01	-1.8993E+01	5.400E-06	5.400E-06	**10%**

Table 3.c. Argon plasma properties of ATMED CR of NLTE-3 workshop

10% hot e- N_e (cm^{-3}) = 10^{23}	Z_{bar} WO hot	Z_{bar} W hot	η_e ATMED CR	ρ W hot (g/cm^3)	ρ WO hot (g/cm^3)
T_e = 100 eV	5.927E+00	4.217E+00	-4.0901E+00	1.580E+00	1.120E+00
T_e = 300 eV	1.458E+01	1.450E+01	-5.7463E+00	4.580E-01	4.580E-01
T_e = 600 eV	1.577E+01	1.573E+01	-6.7868E+00	4.220E-01	4.220E-01
T_e = 1000 eV	1.660E+01	1.651E+01	-7.5464E+00	4.050E-01	4.000E-01
N_e (cm^{-3}) = 10^{23}	Z_{bar} WO hot	Z_{bar} W hot	η_e ATMED CR	ρ W hot (g/cm^3)	% Hot electrons
T_e = 100 eV	5.927E+00	4.217E+00	-4.0901E+00	1.580E+00	10%
T_e = 100 eV	5.927E+00	5.369E+00	-4.0830E+00	1.250E+00	25%
T_e = 100 eV	5.927E+00	8.161E+00	-4.0858E+00	8.200E-01	50%
T_e = 100 eV	5.927E+00	1.208E+01	-4.0932E+00	5.500E-01	75%
T_e = 600 eV	1.577E+01	1.573E+01	-6.7868E+00	4.220E-01	10%
T_e = 600 eV	1.577E+01	1.594E+01	-6.7808E+00	4.190E-01	25%
T_e = 600 eV	1.577E+01	1.637E+01	-6.7832E+00	4.070E-01	50%
T_e = 600 eV	1.577E+01	1.694E+01	-6.7664E+00	4.000E-01	75%

Table 3.d. Argon plasma rates for some levels of ATMED CR of NLTE-3 workshop

N_e (cm^{-3}) = 10^{23}	Coll. Excit. $P_l \rightarrow P_u$	Coll. Excit. Thermal e-	Coll. Excit. Hot e-	Coll. Ion. $P_k \rightarrow c$	Coll. Ion. Thermal e-	Coll. Ion. Hot e-	% Hot electrons
T_e = 100 eV	**25 → 36**	2.794697E+16	8.538635E+14	**1**	1.452343E-04	6.889573E+10	**10%**
T_e = 100 eV	**1 → 18**	1.185290E-04	3.241670E+09	**36**	7.247755E+15	2.577840E+14	**10%**
T_e = 100 eV	**25 → 36**	1.777131E+15	2.309688E+15	**1**	4.623129E-07	4.136981E+11	**75%**
T_e = 100 eV	**1 → 18**	2.182190E-06	5.366048E+10	**36**	6.512641E+13	1.843854E+14	**75%**
T_e = 600 eV	**25 → 36**	3.779647E+15	2.109690E+14	**1**	3.508223E+08	4.964852E+10	**10%**
T_e = 600 eV	**1 → 18**	2.171797E+08	7.340136E+09	**36**	1.685675E+14	1.317161E+13	**10%**
T_e = 600 eV	**25 → 36**	8.935529E+14	1.381487E+15	**1**	7.158341E+07	3.532426E+11	**75%**
T_e = 600 eV	**1 → 18**	4.755530E+07	5.325879E+10	**36**	3.771840E+13	8.403588E+13	**75%**

2.3.2 T_{hot} = 10000 eV at 10% of N_e

Some collisional processes induced by a fraction of 10% very energetic and hot electrons have been also considered at a temperature of T_{hot} = 10 keV, supposing an additive contribution of atomic processes as in Reference of NLTE-4 Workshop [20].

If slight differences in decimal figures are encountered with respect to Reference [20], it is a consequence of having extracted numerical values from files of several options for calculations considering computed electronic density as 1.0E+23, 1.00E+23, 1.000E+18 etc., or convergence limits for relativistic populations 1E-005, 5E-003, etc.

It can be observed that the mean charge is lower for some cases because there are less thermal electrons (90% of a total figure N_e) for promoting bound electrons in excited energy levels up to the continuum. That means, there are 10% hot electrons very energetic producing excitation of electrons in inner shells up to excited energy levels implying a huge jump in energy, but in turn there are 10% less thermal electrons for finally carrying the electrons in excited levels to the continuum.

But increasing for a fixed high temperature as 600 eV, the fraction of hot electrons the mean charge starts to be higher because the percentage increases of hot electrons very energetic producing a lot of excitation of electrons in inner shells up to excited energy levels implying a huge jump in energy. So the number of electrons in excited levels becomes greater and the thermal electrons finally carry them to the continuum. This trend is more peaked for a greater difference between lower and hot temperature (100, 1E+4 eV), being the rates of collisional ionization lower for the inner orbital 1 in respect to thermal electrons at 600 eV. For a high jump in energy of collisional excitation between orbitals 1 → 18, the rate is much lower for thermal electrons at 100 eV in comparison with being at 600 eV, see Appendix I. Hot electrons provide a big rate of collisional excitation in all cases.

2.4 Germanium Plasmas

The following problems have been established for the steady-state cases of germanium atoms on a grid of electron temperatures and electron densities, see Table 4 and Fig. 4:

Element	Case ID	Total # of Points	Parameter	Grid	# of Points
Germanium	Ge	12	T_e	150, 250, 400, 600	4
			N_e	10^{17}, 10^{20}, 3×10^{22}	3

2.4.1 T_{rad} = 0 eV

The cases without a Planckian radiation field are displayed in this section.

Table 4.a. Germanium plasma properties of ATMED CR for comparison with codes of NLTE-3 workshop

N_e (cm^{-3}) = 10^{17}	ρ(g/cm^3)	Z_{bar} ATMED	Z_{bar} NLTE-3	η_e ATMED CR	RPL (1e-7 $J/cm^3/s$)
T_e = 150 eV	1.050E-06	1.152E+01	12÷17.5	-1.8522E+01	3.554017E+14
T_e = 250 eV	9.400E-07	1.327E+01	15÷20	-1.9257E+01	8.083488E+14
T_e = 400 eV	8.452E-07	1.453E+01	17÷22	-1.9978E+01	1.160658E+15
T_e = 600 eV	5.660E-07	2.182E+01	20÷22	-2.0580E+01	3.582530E+14
N_e (cm^{-3}) = 10^{20}	ρ (g/cm^3)	Z_{bar} ATMED	Z_{bar} NLTE-3	η_e ATMED CR	RPL (1e-7 $J/cm^3/s$)
T_e = 150 eV	7.400E-04	1.643E+01	15÷20	-1.1609E+01	7.121588E+19
T_e = 250 eV	6.439E-04	1.874E+01	18÷22	-1.2382E+01	7.559920E+19
T_e = 400 eV	5.922E-04	2.037E+01	20÷22	-1.3088E+01	6.305504E+19
T_e = 600 eV	5.720E-04	2.109E+01	21÷22.5	-1.3696E+01	5.414345E+19
N_e (cm^{-3}) = $3x10^{22}$	ρ (g/cm^3)	Z_{bar} ATMED	Z_{bar} NLTE-3	η_e ATMED CR	RPL (1e-7 $J/cm^3/s$)
T_e = 150 eV	1.969E-01	1.839E+01	17÷20	-5.9112E+00	4.086265E+24
T_e = 250 eV	1.722E-01	2.102E+01	20÷22	-6.6781E+00	2.217217E+24
T_e = 400 eV	1.665E-01	2.174E+01	21.5÷24	-7.3835E+00	2.667664E+24
T_e = 600 eV	1.610E-01	2.247E+01	23÷26	-7.9921E+00	1.254399E+24

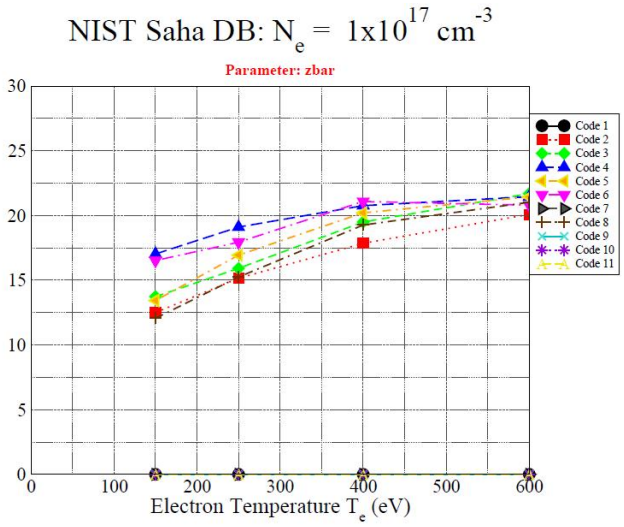

Fig. 4.a. Germanium plasma mean charge computed with codes of NLTE-3 workshop

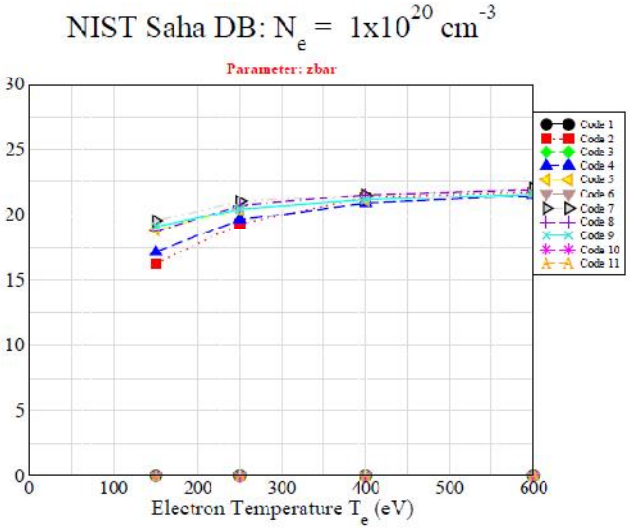

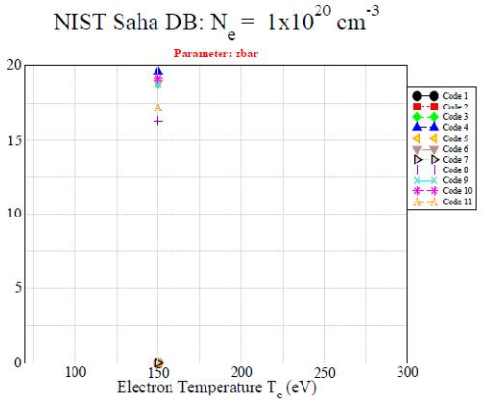

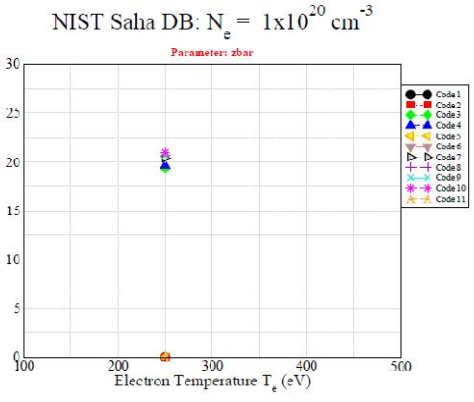

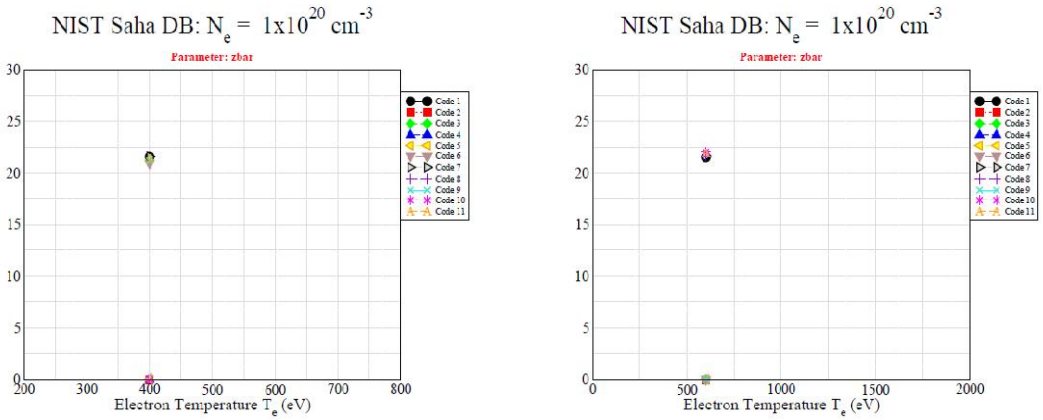

Fig. 4.b. Germanium plasma mean charge of density-temperature points computed with codes of NLTE-3 workshop

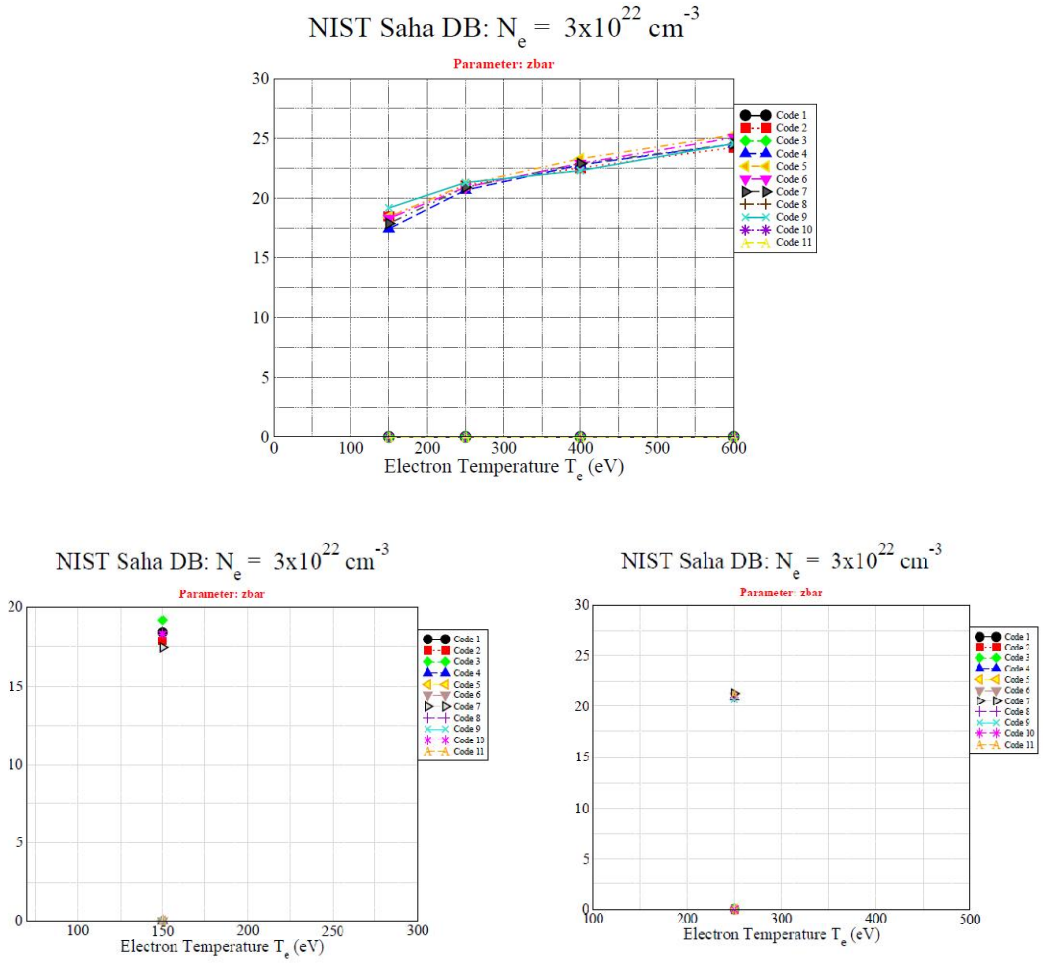

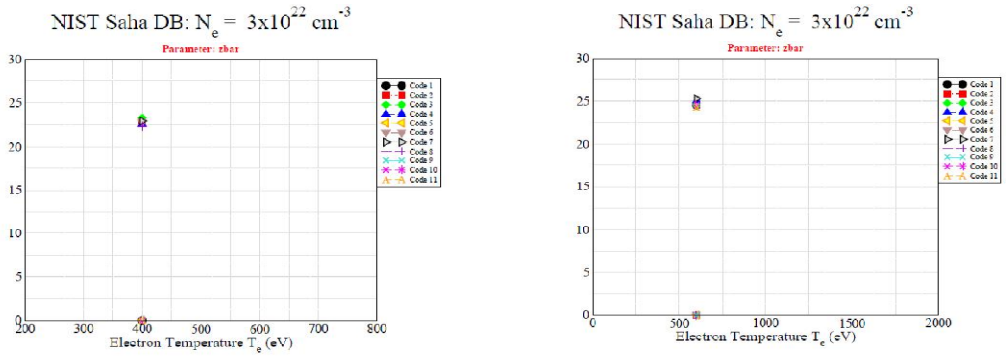

Fig. 4.c. Germanium plasma mean charge of density-temperature points computed with codes of NLTE-3 workshop

2.4.2 $T_{rad} \neq 0$ eV & $N_e = 3x10^{22}$ cm^{-3}

The cases with a Planckian radiation field are displayed in this section.

Element	Case ID	Total # of Points	Parameter	Grid	# of Points
Germanium	GeTr	11	T_e	150, 250, 400, 600	4
			N_e	3×10^{22}	1
			T_{rad}	$T_e/2$, T_e, 300	3

Table 4.b. Germanium plasma properties of ATMED CR for comparison with codes of NLTE-3 workshop at T_{rad} (eV) at N_e = 3E+22 cm^{-3}

$T_{rad} = T_e/2$	Z_{bar} T_{rad} = 0	Z_{bar} $T_{rad} \neq 0$	ρ (g/cm^3)	η_e ATMED CR	RPL (1e-7 J/cm^3/s)
T_e = 150 eV	1.839E+01	1.843E+01	1.964E-01	-5.9113E+00	2.351269E+24
T_e = 250 eV	2.102E+01	2.108E+01	1.717E-01	-6.6784E+00	8.856310E+24
T_e = 400 eV	2.174E+01	2.194E+01	1.649E-01	-7.3837E+00	2.078181E+24
T_e = 600 eV	2.247E+01	2.428E+01	1.491E-01	-7.9915E+00	7.307794E+23
$T_{rad} = T_e$	**Z_{bar} T_{rad} = 0**	**Z_{bar} $T_{rad} \neq 0$**	**ρ (g/cm^3)**	**η_e ATMED CR**	**RPL (1e-7 J/cm^3/s)**
T_e = 150 eV	1.839E+01	1.883E+01	1.922E-01	-5.9114E+00	3.787635E+24
T_e = 250 eV	2.102E+01	2.231E+01	1.622E-01	-6.6784E+00	9.433184E+23
T_e = 400 eV	2.174E+01	2.681E+01	1.350E-01	-7.3836E+00	3.880911E+23
T_e = 600 eV	2.247E+01	2.952E+01	1.226E-01	-7.9917E+00	2.607794E+23
T_{rad} = 300	**Z_{bar} T_{rad} = 0**	**Z_{bar} $T_{rad} \neq 0$**	**ρ (g/cm^3)**	**η_e ATMED CR**	**RPL (1e-7 J/cm^3/s)**
T_e = 150 eV	1.839E+01	2.179E+01	1.700E-01	-5.8885E+00	1.138688E+24
T_e = 250 eV	2.102E+01	2.383E+01	1.550E-01	-6.6580E+00	4.655749E+23
T_e = 400 eV	2.174E+01	2.381E+01	1.520E-01	-7.3836E+00	6.503707E+23
T_e = 600 eV	2.247E+01	2.428E+01	1.491E-01	-7.9915E+00	7.307794E+23

2.4.3 Frequency resolved & mean opacities

The interaction of radiation with matter is determined by the behaviour of electrons in the electromagnetic field of radiation. Depending on the initial and final states of the electron, the code divides the photon absorption processes in three groups: bound-bound, bound-free and free-free transitions. The code ATMED CR performs a calculation of opacities based on the average atom model, where atomic data, binding energies, oscillator strengths, transition probabilities, etc., are obtained from the relativistic screened hydrogenic model. In the formulas for atomic processes, if transitions are or not allowed is implemented through oscillator strengths. The use of several cross sections, quantum or reduced, has been tested, considering as a reference the opacity calculated by the code ATMED LTE, where the mean charge and the populations are practically equal to ones computed after solving the CR balance for a plasma in LTE regime. And now the cross sections used are indicated in schematic form, detailing their meaning in the references. There are two absorption cross sections of the radiation field in spectral lines for bound-bound transitions between relativistic orbitals:

- Bound-Bound Absorption Cross Section (Rozsnyai-Nikiforov [12-14]) ~ Mixed UTA:

$$\sigma_{bb}(h\nu) = 2\pi^2 \alpha a_0 e^2 f_{kk'} S_{kk'}(h\nu) \tag{1}$$

- Bound-Bound Absorption Cross Section ([5]) ~ UTA/STA:

$$\sigma^{bb}_{kk'}(h\nu) = \frac{\pi h e^2}{m_e c} \sum_{kk'} P_k \; f_{kk'} S_{kk'}(h\nu) \tag{2}$$

where:

$f_{kk'}$: Photon absorption oscillator strength for the transition from the orbital k to other k' developed in Laguerre polynomials and based on wavefunctions constructed with relativistic screened charges [5-7].

$S_{kk'}(h\nu)$: Voigt profile which includes Doppler, Natural, Stark and Dielectronic broadenings.

The first, Equation (1), provides a discrete structure of lines which retains in the spectrum the lines of high intensity between the relativistic orbitals of the average atom which represents the plasma, being equivalent to apply the formalism MUTA (Mixed Unresolved Transition Array) in the spectrum calculated by a detailed code [9]. The second, Equation (2), is the average of the first one Equation (1), which provides general characteristics of the absorption spectrum being equivalent to apply the formalism UTA (Unresolved Transition Array). It is considered also the dielectronic broadening which implies the statistical grouping of lines computing greater values of Rosseland mean opacity, being very sensitive to the regions of low opacity in the frequency resolved spectrum. The UTA spectral structures are sometimes shifted in photon energy with respect to detailed spectra of DLA/DTA codes as density increases due to more separated lines of the same array of electronic transitions. Depending on the calculated plasma, a greater or lower degree of agreement between UTA and MUTA formalisms is obtained in the order of magnitude of Rosseland (K_R) and Planck (K_P) mean opacities. The greater the density, the better the concordance of figures of K_R. The values of K_P are in good agreement for practically all displayed plasma cases.

The greater the temperature at high density as 3 x 10^{22} cm^{-3}, the bigger the departure between computing with UTA formalism considering T_e = T_{rad} or T_{rad} = 0 eV, see Figs. 4d÷4f.

Table 4.c. Germanium plasma mean opacities of ATMED CR UTA or MUTA of NLTE-3 workshop at T_{rad} (eV)

T_e = 250 eV &	N_e = 1E+17 cm^{-3}	K_R UTA (cm^2/g)	K_R MUTA (cm^2/g)	K_P UTA (cm^2/g)	K_P MUTA (cm^2/g)
T_{rad} = 0		1.425E+03	1.241E+02	3.797E+03	2.745E+03
T_e = 250 eV &	N_e = 1E+20 cm^{-3}	K_R UTA (cm^2/g)	K_R MUTA (cm^2/g)	K_P UTA (cm^2/g)	K_P MUTA (cm^2/g)
T_{rad} = 0		8.835E+02	1.049E+02	2.518E+03	2.182E+03
T_e = 400 eV &	N_e = 1E+17 cm^{-3}	K_R UTA (cm^2/g)	K_R MUTA (cm^2/g)	K_P UTA (cm^2/g)	K_P MUTA (cm^2/g)
T_{rad} = 0		8.425E+02	9.233E+01	2.952E+03	2.174E+03
T_e = 400 eV &	N_e = 1E+20 cm^{-3}	K_R UTA (cm^2/g)	K_R MUTA (cm^2/g)	K_P UTA (cm^2/g)	K_P MUTA (cm^2/g)
T_{rad} = 0		5.854E+02	7.913E+01	2.321E+03	1.999E+03
T_e = 600 eV &	N_e = 1E+17 cm^{-3}	K_R UTA (cm^2/g)	K_R MUTA (cm^2/g)	K_P UTA (cm^2/g)	K_P MUTA (cm^2/g)
T_{rad} = 0		1.230E+01	1.415E+00	1.766E+03	1.397E+03
T_e = 600 eV &	N_e = 1E+20 cm^{-3}	K_R UTA (cm^2/g)	K_R MUTA (cm^2/g)	K_P UTA (cm^2/g)	K_P MUTA (cm^2/g)

T_{rad} = 0		3.527E+02	7.229E+01	1.793E+03	1.490E+03
T_e = 150 eV &	N_e = 3E+22 cm^{-3}	K_R UTA (cm^2/g)	K_R MUTA (cm^2/g)	K_P UTA (cm^2/g)	K_P MUTA (cm^2/g)
T_{rad} = 0		1.133E+03	6.893E+02	3.349E+03	3.268E+03
T_{rad} = T_e/2		2.288E+03	1.085E+03	6.623E+03	6.130E+03
T_{rad} = 300 eV		3.311E+02	1.378E+02	1.857E+03	1.730E+03
T_{rad} = T_e		9.896E+02	6.147E+02	3.089E+03	3.017E+03
T_e = 250 eV &	N_e = 3E+22 cm^{-3}	K_R UTA (cm^2/g)	K_R MUTA (cm^2/g)	K_P UTA (cm^2/g)	K_P MUTA (cm^2/g)
T_{rad} = 0		3.625E+02	1.858E+02	1.823E+03	1.700E+03
T_{rad} = T_e/2		3.902E+02	3.013E+02	2.026E+03	1.881E+03
T_{rad} = 300 eV		1.274E+02	5.841E+01	1.341E+03	1.286E+03
T_{rad} = T_e		1.796E+02	9.895E+01	1.428E+03	1.345E+03
T_e = 400 eV &	N_e = 3E+22 cm^{-3}	K_R UTA (cm^2/g)	K_R MUTA (cm^2/g)	K_P UTA (cm^2/g)	K_P MUTA (cm^2/g)
T_{rad} = 0		3.708E+02	1.246E+02	2.064E+03	1.878E+03
T_{rad} = T_e/2		1.991E+02	1.423E+02	1.229E+03	1.174E+03
T_{rad} = 300 eV		1.421E+02	6.575E+01	1.357E+03	1.308E+03
T_{rad} = T_e		7.595E+01	2.881E+01	8.314E+02	8.195E+02
T_e = 600 eV &	N_e = 3E+22 cm^{-3}	K_R UTA (cm^2/g)	K_R MUTA (cm^2/g)	K_P UTA (cm^2/g)	K_P MUTA (cm^2/g)
T_{rad} = 0		3.071E+02	1.028E+02	1.580E+03	1.390E+03
T_{rad} =T_e/2=300 eV		1.262E+02	6.030E+01	1.248E+03	1.217E+03
T_{rad} = T_e		1.120E+01	6.740E+00	1.156E+02	1.153E+02

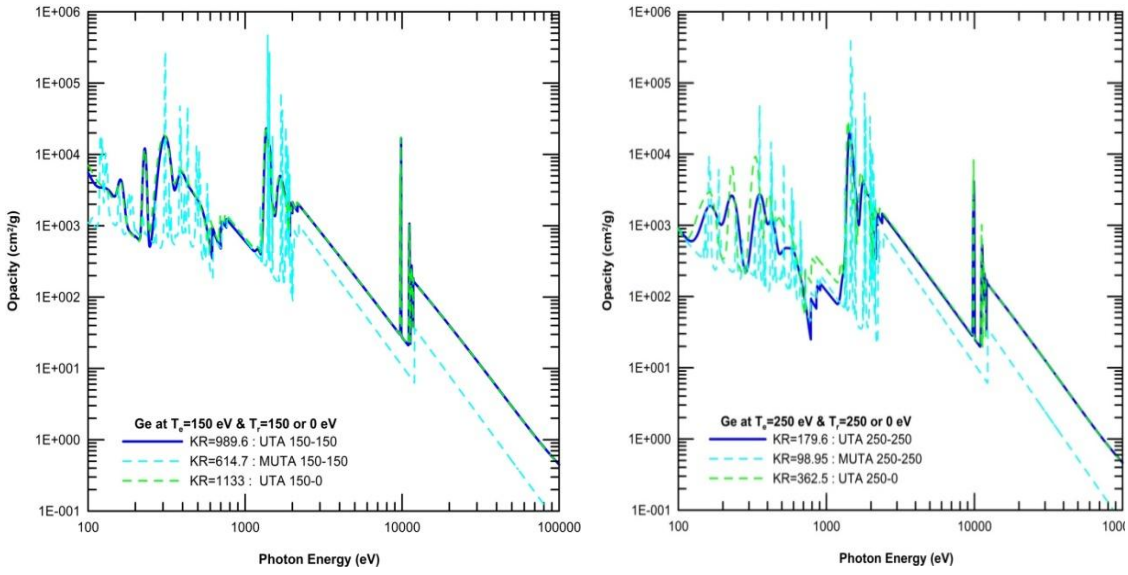

Fig. 4.d. Frequency resolved opacity of germanium plasma at density 3E+22 cm^{-3} with ATMED CR at T_{rad} = 150 eV in UTA (—) or MUTA (—) formalisms or T_{rad} = 0 eV in UTA (—) formalism and T_e = 150 eV observing the sensitivity to departures from LTE regime (left). Germanium plasma frequency resolved opacity of ATMED CR at T_{rad} = 250 eV in UTA (—) or MUTA (—) formalisms or T_{rad} = 0 eV in UTA (—) formalism and T_e = 250 eV observing the sensitivity to departures from LTE regime (right)

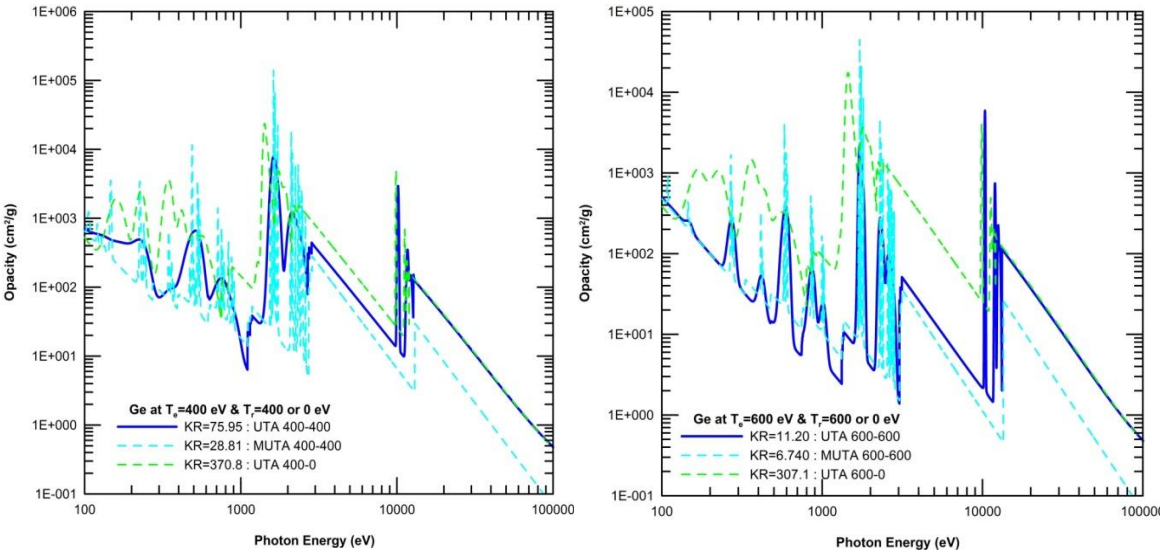

Fig. 4.e. Frequency resolved opacity of germanium plasma at density 3E+22 cm^{-3} with ATMED CR at T_{rad} = 400 eV in UTA (—) or MUTA (—) formalisms or T_{rad} = 0 eV in UTA (—) formalism and T_e = 400 eV observing the sensitivity to departures from LTE regime (left). Germanium plasma frequency resolved opacity of ATMED CR at T_{rad} = 600 eV in UTA (—) or MUTA (—) formalisms or T_{rad} = 0 eV in UTA (—) formalism and T_e = 600 eV observing the sensitivity to departures from LTE regime (right)

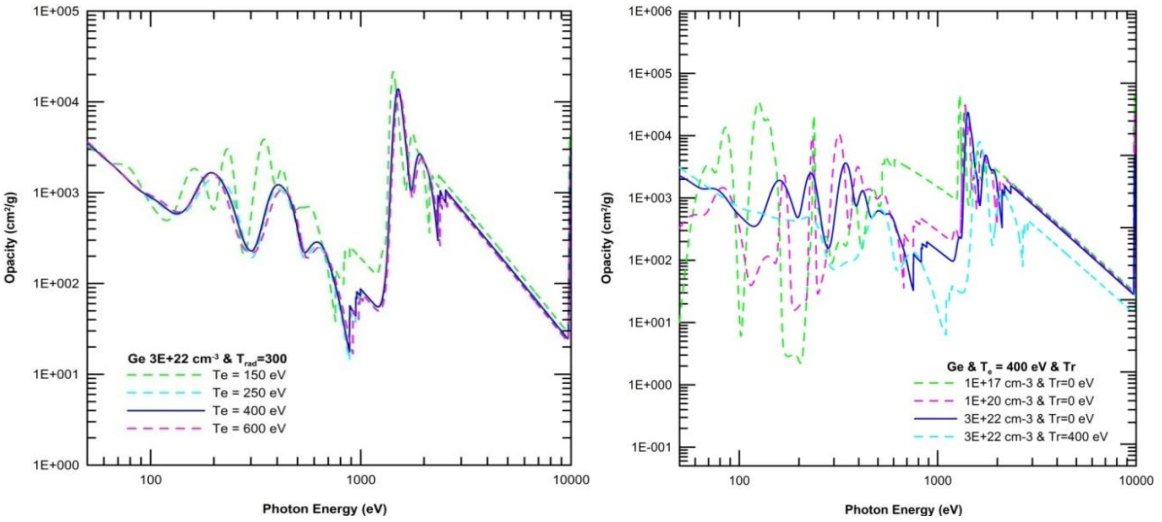

Fig. 4.f. Germanium plasma frequency resolved opacity of ATMED CR at T_{rad} = 300 eV and T_e = 150 (—), 250 (—), 400 (—) and 600 (—) eV observing the sensitivity to electronic temperature variation (left). Germanium plasma properties of ATMED CR at T_{rad} = 0 eV, T_e = 400 eV (—) at N_e = 3E+22 cm^{-3}; T_{rad} = T_e = 400 eV (—) at N_e = 3E+22 cm^{-3} and T_e = 400 eV and densities N_e = 1E+17 (—), 1E+20 (—) cm^{-3} at T_{rad} = 0 eV observing the sensitivity to density and radiation temperature variations (right)

2.5 Xenon Plasmas

The following problems have been established for the steady-state cases of xenon atoms on a grid of electron temperatures and electron densities, see Table 5 and Fig. 5:

It can be observed for xenon plasmas created in LULI facility [21], the appreciable difference in

this element plasma properties, especially for mean charge, depending on if it is used the maximum principal quantum number n_{max}= 6 or 10.

Element	Case ID	Total # of Points	Parameter	Grid	# of Points
Xenon	Xe	6	T_e	200, 375, 415, 455, 600, 750	6
			N_i (ion!)	4.75×10^{18}	1
			Spectrum	9–120 Å	2221

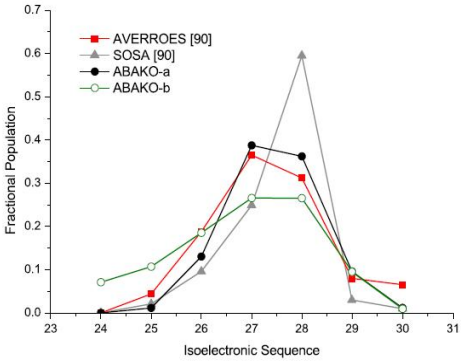

TABLE VII. Average ionization for the Xe plasma created at LULI [96] and calculations obtained by different models. For ABAKO and AVERROES the ion density $n_{ion}=4.75\times10^{18}$ cm^{-3} and T_e=450 eV are input parameters. For the SOSA fit a value of T_e =400 eV was assumed.

Source	$\bar{Z}$
Experiment [96]	27.4 ± 1.5
ABAKO-a	26.6
ABAKO-b	27.1
AVERROES [96]	26.8
SOSA fit [96]	26.5

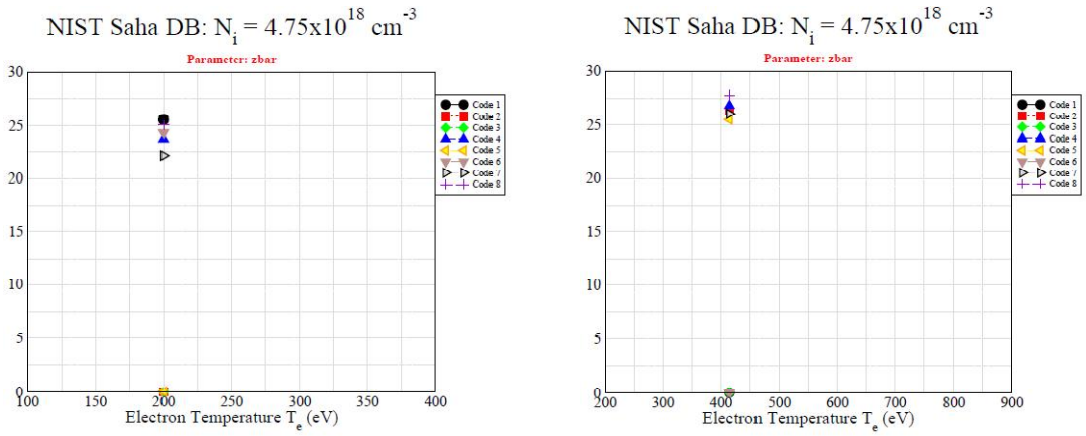

Fig. 5.a. Charge state distributions simulated by CR detailed models for xenon experiment carried out in LULI facility [21]. Mean charge of xenon created in LULI facility. Calculations obtained for N_i=4.75x10^{18} cm^{-3} and T_e=450 eV

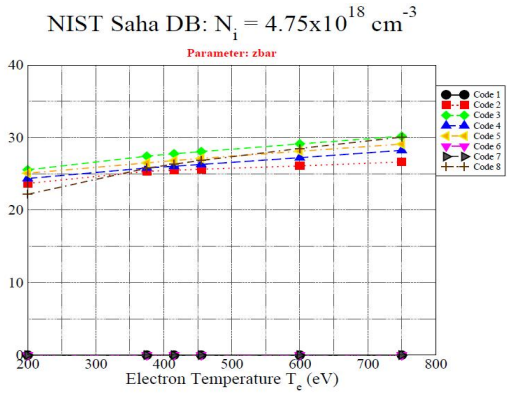

Fig. 5.b. Xenon plasma mean charge computed with codes of NLTE-3 workshop

Table 5. Xenon plasma properties of ATMED CR for comparison with codes of NLTE-3 workshop

T_e (eV) = 200	ρ (g/cm^3)	N_e (cm^{-3})	N_{ion} (ion.cm^{-3})	Z_{bar} NLTE-3	Z_{bar} ATMED	RPL (J/cm^3/s)
n_{max} = 6	1.0356E-03	1.162E+20	4.750E+18	22÷25.5	2.447E+01	1.583445E+13
n_{max} = 10	1.0356E-03	1.246E+20	4.750E+18	22÷25.5	2.624E+01	2.991353E+15
T_e (eV) = 375	ρ (g/cm^3)	N_e (cm^{-3})	N_{ion} (ion.cm^{-3})	Z_{bar} NLTE-3	Z_{bar} ATMED	RPL (J/cm^3/s)
n_{max} = 6	1.0356E-03	1.217E+20	4.750E+18	25÷27.5	2.561E+01	1.568357E+13
n_{max} = 10	1.0356E-03	1.406E+20	4.750E+18	25÷27.5	2.959E+01	1.081961E+15
T_e (eV) = 415	ρ (g/cm^3)	N_e (cm^{-3})	N_{ion} (ion.cm^{-3})	Z_{bar} NLTE-3	Z_{bar} ATMED	RPL (J/cm^3/s)
n_{max} = 6	1.0356E-03	1.223E+20	4.750E+18	25÷27.5	2.575E+01	1.510424E+13
n_{max} = 10	1.0356E-03	1.438E+20	4.750E+18	25÷27.5	3.028E+01	7.868060E+15
T_e (eV) = 455	ρ (g/cm^3)	N_e (cm^{-3})	N_{ion} (ion.cm^{-3})	Z_{bar} NLTE-3	Z_{bar} ATMED	RPL (J/cm^3/s)
n_{max} = 6	1.0356E-03	1.229E+20	4.750E+18	25.5÷28	2.587E+01	1.557981E+13
n_{max} = 10	1.0356E-03	1.464E+20	4.750E+18	25.5÷28	3.082E+01	4.913842E+15
T_e (eV) = 600	ρ (g/cm^3)	N_e (cm^{-3})	N_{ion} (ion.cm^{-3})	Z_{bar} NLTE-3	Z_{bar} ATMED	RPL (J/cm^3/s)
n_{max} = 6	1.0356E-03	1.247E+20	4.750E+18	26÷29	2.625E+01	1.830720E+13
n_{max} = 10	1.0356E-03	1.525E+20	4.750E+18	26÷29	3.210E+01	8.147788E+15
T_e (eV) = 750	ρ (g/cm^3)	N_e (cm^{-3})	N_{ion} (ion.cm^{-3})	Z_{bar} NLTE-3	Z_{bar} ATMED	RPL (J/cm^3/s)
n_{max} = 6	1.0356E-03	1.264E+20	4.750E+18	26÷30.5	2.661E+01	1.944406E+13
n_{max} = 10	1.0356E-03	1.578E+20	4.750E+18	26÷30.5	3.322E+01	9.224302E+14

2.6 Gold Plasmas

The following problems have been established for the steady-state cases of gold atoms on a grid of electron temperatures and electron densities. See Table 6 and Fig. 6:

If the upper limit used in autoionization is 10^{14} s^{-1} at high temperatures the values in Table 6 are obtained. Greater values more centered in the range of codes for higher temperatures can be computed with other formulas with upper limit of the order of magnitude 10^{17} s^{-1} [22,23].

Element	Case ID	Total # of Points	Parameter	Grid	# of Points
Gold	Au	18	T_e	750, 1500, 2500	3
			N_e	10^{19}, 10^{20}, 10^{21}, 10^{22}, 10^{23}, 10^{24}	6

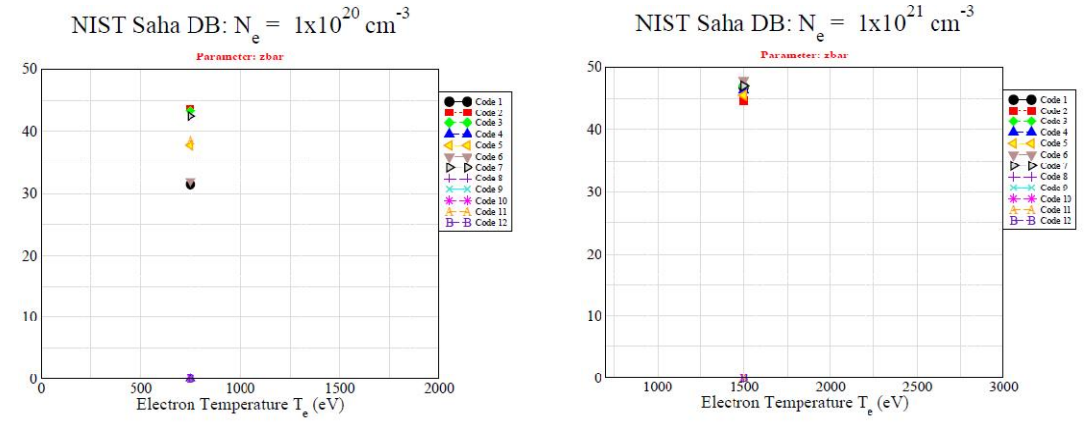

Fig. 6.a. Gold plasma mean charge computed with codes of NLTE-3 workshop

Table 6.a. Gold plasma properties of ATMED CR for comparison with codes of NLTE-3 workshop

N_e (cm^{-3}) = 10^{19}	ρ (g/cm^3)	Z_{bar} ATMED	Z_{bar} NLTE-3	η_e ATMED CR	RPL (1e-7 $J/cm^3/s$)
T_e = 750 eV	1.260E-04	2.670E+01	27÷43	-1.6305E+01	4.261264E+19
T_e = 1500 eV	9.154E-05	3.573E+01	39÷46	-1.7373E+01	3.316573E+19
T_e = 2500 eV	7.418E-05	4.409E+01	44÷50	-1.8139E+01	2.809442E+19
N_e (cm^{-3}) = 10^{20}	ρ (g/cm^3)	Z_{bar} ATMED	Z_{bar} NLTE-3	η_e ATMED CR	RPL (1e-7 $J/cm^3/s$)
T_e = 750 eV	1.100E-03	3.074E+01	30÷45	-1.3997E+01	8.934351E+20
T_e = 1500 eV	8.420E-04	3.890E+01	40÷47	-1.5069E+01	1.838753E+21
T_e = 2500 eV	7.200E-04	4.564E+01	45÷50	-1.5832E+01	2.339277E+21
N_e (cm^{-3}) = 10^{21}	ρ (g/cm^3)	Z_{bar} ATMED	Z_{bar} NLTE-3	η_e ATMED CR	RPL (1e-7 $J/cm^3/s$)
T_e = 750 eV	9.026E-03	3.625E+01	34÷45	-1.1728E+01	5.307210E+22
T_e = 1500 eV	7.540E-03	4.345E+01	44÷50	-1.2766E+01	8.309760E+22
T_e = 2500 eV	6.950E-03	4.718E+01	47÷50	-1.3532E+01	7.744388E+22

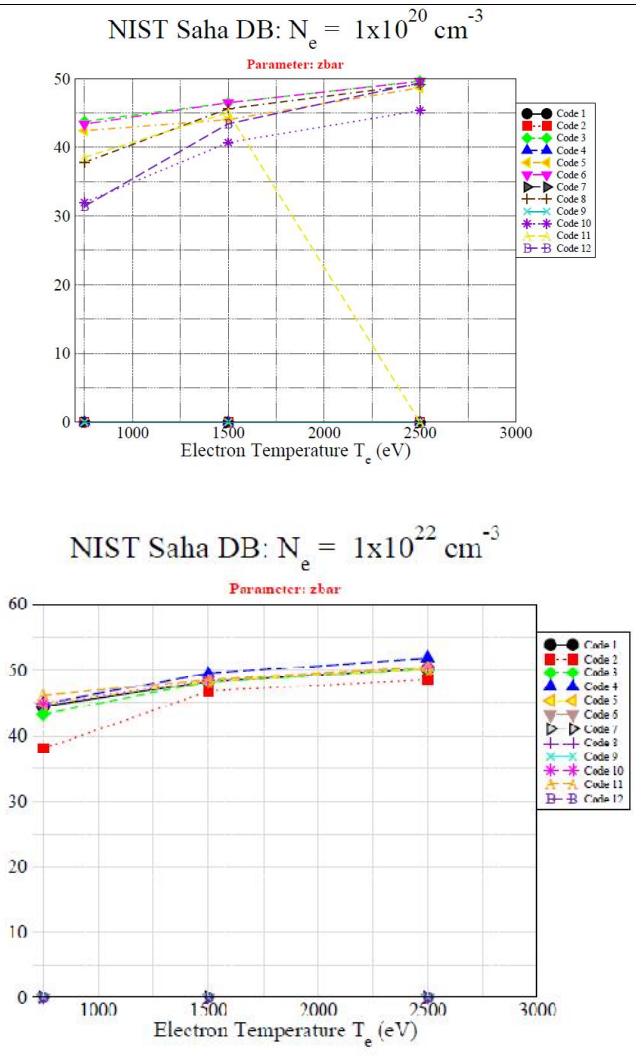

Fig. 6.b. Gold plasma mean charge computed with codes of NLTE-3 workshop

Table 6.b. Gold plasma properties of ATMED CR for comparison with codes of NLTE-3 workshop

N_e (cm^{-3}) = 10^{22}	ρ (g/cm^3)	Z_{bar} ATMED	Z_{bar} NLTE-3	η_e ATMED CR	RPL (1e-7 $J/cm^3/s$)
T_e = 750 eV	7.884E-02	4.149E+01	37÷48	-9.4252E+00	1.211432E+24
T_e = 1500 eV	7.143E-02	4.579E+01	45÷51	-1.0465E+01	2.032188E+24
T_e = 2500 eV	6.748E-02	4.847E+01	46÷54	-1.1231E+01	1.100801E+24

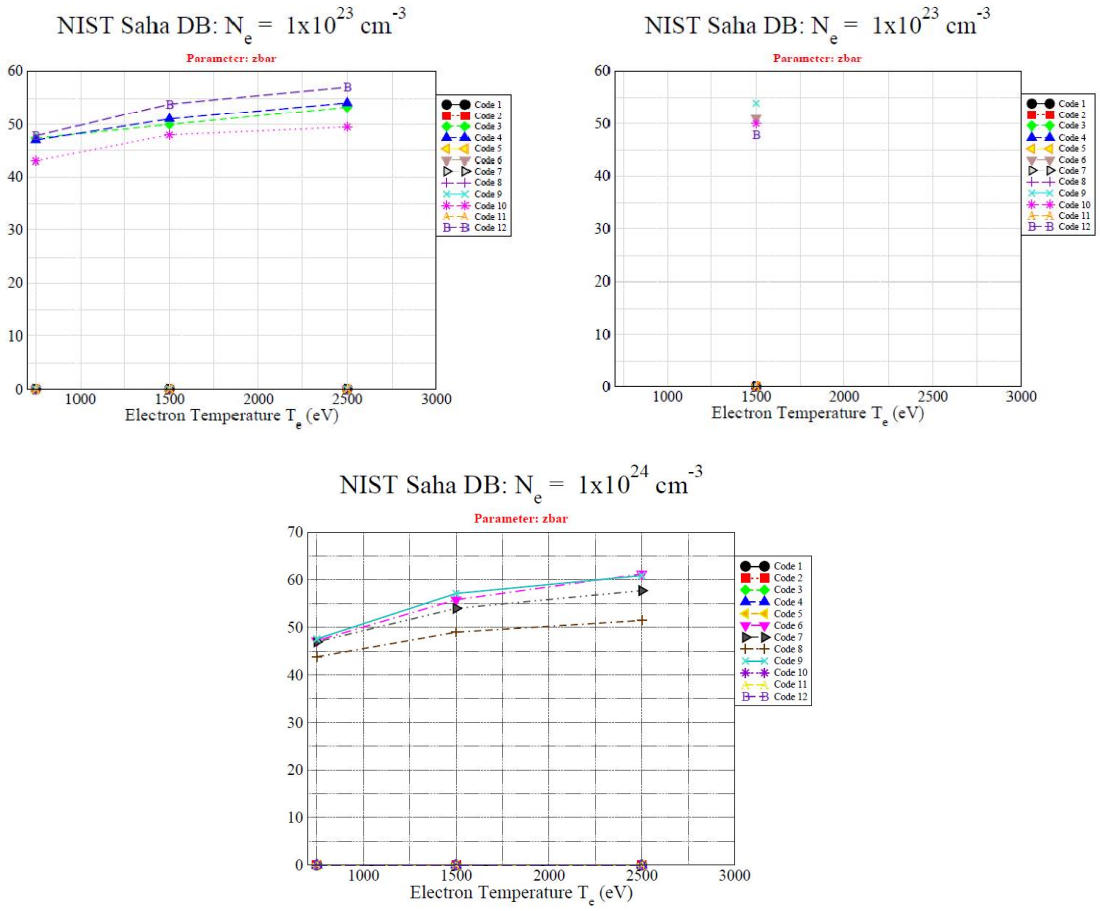

Fig. 6.c. Gold plasma mean charge computed with codes of NLTE-3 workshop

Table 6.c. Gold plasma properties of ATMED CR for comparison with codes of NLTE-3 workshop

N_e (cm^{-3}) = 10^{23}	ρ (g/cm^3)	Z_{bar} ATMED	Z_{bar} NLTE-3	η_e ATMED CR	RPL (1e-7 $J/cm^3/s$)
T_e = 750 eV	7.549E-01	4.334E+01	42÷50	-7.1223E+00	1.127530E+27
T_e = 1500 eV	6.899E-01	4.741E+01	47÷55	-8.1624E+00	4.921110E+25
T_e = 2500 eV	6.501E-01	5.031E+01	49÷59	-8.9288E+00	4.974738E+25
N_e (cm^{-3}) = 10^{24}	ρ (g/cm^3)	Z_{bar} ATMED	Z_{bar} NLTE-3	η_e ATMED CR	RPL (1e-7 $J/cm^3/s$)
T_e = 750 eV	7.806E+00	4.193E+01	43÷49	-4.8167E+00	4.216810E+27
T_e = 1500 eV	6.682E+00	4.896E+01	48÷58	-5.8588E+00	2.782662E+28
T_e = 2500 eV	6.060E+00	5.427E+01	50÷62	-6.6203E+00	4.795663E+27

2.7 Germanium Time Dependent Plasma

The following problem has been established for the temporal case of germanium X-ray laser plasma, see Table 7 and Fig. 7. In Appendix II it is shown the time history of T_e (left hand axis) and N_e (right hand axis) for the TD-Ge case, which is motivated by the germanium X-ray laser experiments.

This calculation should be carried out to t = 1.975 ns, and the exigent non-uniform time grid along with the corresponding values of T_e and N_e are presented in Appendix II. The initial condition is LTE. In order not to entering in an infinite iterative loop or interrupted execution of FORTRAN code, the following criteria have been used for calculation with ATMED CR, considering matter density as the fundamental parameter for computation:

- There is a first loop of convergence in electronic density with criteria 1E-03, for coincidence up to the second decimal figure at least followed by power E+20, with input parameter the N_e of the provided grid.
- There is a second loop inside the previous one of convergence in populations of electronic relativistic orbitals with criteria 1E-02 or more strict 5E-04, obtaining times of CPU computation of 5.610016E+03 or 1.742531E+04 seconds respectively, this means 1.558 or 4.84 hours:
    - The computation with code ATMED CR starts at step 14 with conditions:

Step #	Time (s)	Te	Ne
14	5.3137E-10	2.0025E+02	2.4230E+20

    - The computation with code ATMED CR ends at step 82 with conditions:

Step #	Time (s)	Te	Ne
82	1.9749E-09	3.4240E+02	1.2526E+20

- Relaxing even more the convergence criteria for populations up to 1.5E-02, CPU time is 3.978703E+03 s (1.105 h) and the computation with ATMED CR can start at step 11:

Step #	Time (s)	Te	Ne
11	4.7441E-10	8.2758E+01	2.2823E+20

Some results are displayed in Appendix II, Fig. 7 and Table 7, being the acronyms as follows:

- **BB, BF, FF and Total RPL** Bound-Bound, Bound-Free, Free-Free and Total Radiative Power Losses in J/(cm^3.s).
- **<S_{tot}>** The total ionization rate out of the average atom. This quantity is further summed over all ionization processes.
- **<f_S_{coll}>** The fractional contribution of electron collisional ionization processes to **<S_{tot}>.**
- **<f_S_{photo}>** The fractional contribution of photo-ionization processes to **<S_{tot}>.**
- **<f_S_{auto}>** The fractional contribution of auto-ionization processes to **<S_{tot}>**.
- **<α_{tot}>** The total recombination rate of the average atom. This quantity is further summed over all recombination processes.
- **<f_α_{coll}>** The fractional contribution of three-body recombination to the total **<α_{tot}>**.
- **<f_α_{photo}>** The fractional contribution of radiative-recombination to the total **<α_{tot}>**.
- **<f_α_{auto}>** The fractional contribution of dielectronic capture processes to the total **<α_{tot}>**.
- **<Γ_{tot}>** The total population flux out of the average atom. Units are s^{-1}.
- **<f_Γ_{collBB}>** The fractional contribution of electron collision excitation/de-excitation processes to **<Γ_{tot}>**.

- **<f_$\Gamma_{photoBB}$>** The fractional contribution of bound-bound radiation processes to **<Γ_{tot}>**.
- **<f_Γ_{collBF}>** The fractional contribution of electron collision ionization processes to **<Γ_{tot}>**.
- **<f_$\Gamma_{photoBF}$>** The fractional contribution of photo-ionization to **<Γ_{tot}>**.
- **<f_Γ_{auto}>** The fractional contribution of auto-ionization/dielectronic recombination processes to **<Γ_{tot}>**.
- **<Θ_{tot}>** The total population flux into the average atom. Units are s^{-1}.
- **<f_Θ_{collBB}>** The fractional contribution of electron collision excitation/de-excitation processes to **<Θ_{tot}>**.
- **<f_$\Theta_{photoBB}$>** The fractional contribution of bound-bound radiation processes to **<Θ_{tot}>**.
- **<f_Θ_{collBF}>** The fractional contribution of electron collision recombination processes to **<Θ_{tot}>**.
- **<f_$\Theta_{photoBF}$>** The fractional contribution of photo-recombination to **<Θ_{tot}>**.
- **<f_Θ_{auto}>** The fractional contribution of auto-ionization/dielectronic recombination processes to **<Θ_{tot}>**.
- **<occ1>, <occ2>, etc.** Fractional occupation number of electrons in the K shell, L shell, etc. of the average atom.

In Appendix II it is shown the whole time history of mean charge, matter and ionic density and relativistic orbital populations in the average atom for all temporal intervals. In Table 2.d it is displayed the electronic density after computation used by ATMED CR versus the input value of N_e. With this code it is observed in figures of columns <occ2>, <occ3> of Table 2.e-f-g, that the depletion of L-shell and M-Shell with 8 and 18 electronic positions is extremely rapid, occurring at temporal intervals 8.477300E-10 and 5.313700E-10 seconds, respectively.

In Appendix II, Fig. 7 and Table 7, it is also observed that good results are still maintained even for less strict criteria of convergence in the loop of populations as < 1E-02, computing in much lower CPU time (1.558 < 4.84 h) an optimal whole time history of mean charge, matter and ionic density and relativistic orbital populations in the average atom.

Table 7.a. Germanium plasma properties of ATMED CR for 4 temporal representative intervals with criteria of convergence in populations of < 1E-02

Step	Time (s)	BB RPL	BF RPL	FF RPL	Total RPL
14	5.313700E-10	1.869183E+11	4.870430E+05	8.036349E+07	1.869991E+11
36	8.657700E-10	1.600383E+10	1.458753E+05	4.774089E+07	1.605172E+10
58	1.084400E-09	4.094735E+09	1.116198E+05	3.547699E+07	4.130324E+09
82	1.974900E-09	8.684380E+07	1.870771E+05	2.155397E+07	1.085848E+08
Step	**Time (s)**	**<S_{tot}>**	**<f_S_{coll}>**	**<f_S_{photo}>**	**<f_S_{auto}>**
14	5.313700E-10	1.014657E+16	8.384767E-05	0.000000E+00	9.999162E-01
36	8.657700E-10	9.931239E+14	8.173540E-04	0.000000E+00	9.991826E-01
58	1.084400E-09	8.198916E+14	8.470501E-04	0.000000E+00	9.991529E-01
82	1.974900E-09	3.044400E+13	6.215985E-03	0.000000E+00	9.937840E-01
Step	**Time (s)**	**<α_{tot}>**	**<f_α_{coll}>**	**<f_α_{photo}>**	**<f_α_{auto}>**
14	5.313700E-10	2.364472E+12	1.674265E-05	0.000000E+00	9.999833E-01
36	8.657700E-10	1.805011E+10	8.095559E-05	0.000000E+00	9.999190E-01
58	1.084400E-09	5.991476E+09	1.762400E-04	0.000000E+00	9.998238E-01
82	1.974900E-09	1.417566E+07	1.470520E-01	0.000000E+00	8.529480E-01

Table 7.b. Germanium plasma properties of ATMED CR for 4 temporal representative intervals with criteria of convergence in populations of < 1E-02

Time (s)	<Γ_{tot}>	<f_Γ_{collBB}>	<f_$\Gamma_{photoBB}$>	<f_Γ_{collBF}>	<f_$\Gamma_{photoBF}$>	<f_Γ_{auto}>
5.313700E-10	1.345911E+16	2.452333E-01	0.000000E+00	6.321120E-05	0.000000E+00	7.547035E-01
8.657700E-10	2.325453E+15	5.714696E-01	0.000000E+00	3.490649E-04	0.000000E+00	4.281813E-01
1.084400E-09	1.974015E+15	5.831757E-01	0.000000E+00	3.518155E-04	0.000000E+00	4.164724E-01
1.974900E-09	1.203081E+15	9.720865E-01	0.000000E+00	1.572956E-04	0.000000E+00	2.775621E-02
Time (s)	**<Θ_{tot}>**	**<f_Θ_{collBB}>**	**<f_$\Theta_{photoBB}$>**	**<f_Θ_{collBF}>**	**<f_$\Theta_{photoBF}$>**	**<f_Θ_{auto}>**
5.313700E-10	1.214971E+18	5.176583E-06	0.000000E+00	3.258312E-11	0.000000E+00	9.999948E-01
8.657700E-10	2.805846E+12	1.088537E-02	0.000000E+00	5.207904E-07	0.000000E+00	9.891141E-01
1.084400E-09	6.179158E+10	1.171259E-01	0.000000E+00	1.708870E-05	0.000000E+00	8.828570E-01
1.974900E-09	6.572407E+08	8.989837E-01	0.000000E+00	3.171684E-03	0.000000E+00	9.784461E-02
Time (s)	**<occ1>**	**<occ2>**	**<occ3>**	**<occ4>**	**<occ5>**	**<occ6>**
5.313700E-10	1.996457	7.135317	0.043153	0.007621	0.002039	0.000068
8.657700E-10	1.994999	0.014036	0.000737	0.000538	0.000236	0.000012
1.084400E-09	1.900191	0.001187	0.000206	0.000182	0.000083	0.000004
1.974900E-09	1.892914	0.000016	0.000015	0.000016	0.000008	0.000000

Table 7.c. Germanium plasma properties of ATMED CR for 4 temporal representative intervals with criteria of convergence in populations of < 5E-04

Step	Time (s)	BB RPL	BF RPL	FF RPL	Total RPL
14	5.313700E-10	1.158548E+11	5.662678E+05	8.194356E+07	1.159373E+11
36	8.657700E-10	9.976331E+09	1.467755E+05	4.775693E+07	1.002423E+10
58	1.084400E-09	3.962199E+09	1.121020E+05	3.548255E+07	3.997794E+09
82	1.974900E-09	6.932130E+07	1.879786E+05	2.155841E+07	9.106769E+07
Step	**Time (s)**	**<S_{tot}>**	**<f_S_{coll}>**	**<f_S_{photo}>**	**<f_S_{auto}>**
14	5.313700E-10	1.148174E+16	5.944060E-05	0.000000E+00	9.999406E-01
36	8.657700E-10	7.561204E+14	1.070497E-03	0.000000E+00	9.989295E-01
58	1.084400E-09	8.316737E+14	8.339985E-04	0.000000E+00	9.991660E-01
82	1.974900E-09	2.316033E+13	8.153805E-03	0.000000E+00	9.918462E-01
Step	**Time (s)**	**<α_{tot}>**	**<f_α_{coll}>**	**<f_α_{photo}>**	**<f_α_{auto}>**
14	5.313700E-10	1.815799E+12	1.912149E-05	0.000000E+00	9.999809E-01
36	8.657700E-10	9.365499E+09	1.556759E-04	0.000000E+00	9.998443E-01
58	1.084400E-09	5.904197E+09	1.786681E-04	0.000000E+00	9.998213E-01
82	1.974900E-09	1.091453E+07	1.907511E-01	0.000000E+00	8.092489E-01

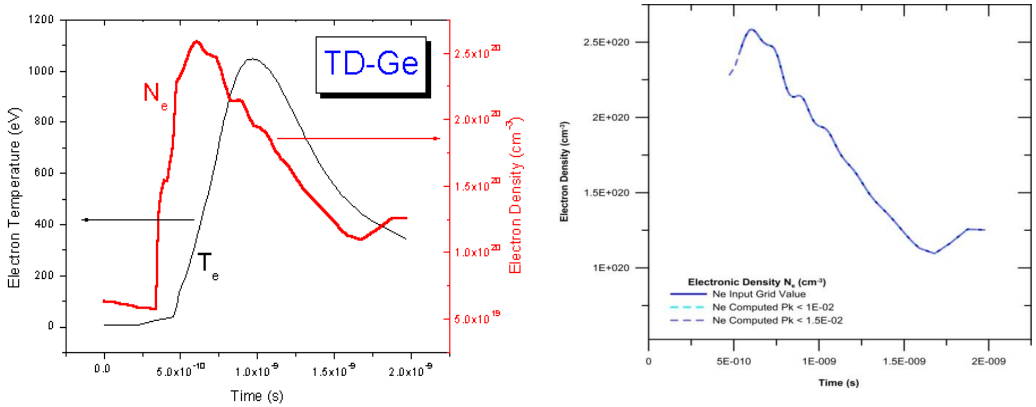

Fig. 7.a. Time history of plasma parameters for TD-Ge provided by workshop NLTE-3 (left). Profiles used by ATMED CR: electronic density as input parameter and computed electronic density with criteria of convergence 1E-03 for matching each value of electronic density as input parameter at the belonging temporal interval (right), with criteria of convergence in populations of < 1.5 E-02 and < 1 E-02

Table 7.d. Germanium plasma properties of ATMED CR for 4 temporal representative intervals with criteria of convergence in populations of < 5E-04

Time (s)	$<\Gamma_{tot}>$	$<f\_\Gamma_{collBB}>$	$<f\_\Gamma_{photoBB}>$	$<f\_\Gamma_{collBF}>$	$<f\_\Gamma_{photoBF}>$	$<f\_\Gamma_{auto}>$
5.313700E-10	1.456945E+16	2.112005E-01	0.000000E+00	4.684334E-05	0.000000E+00	7.887527E-01
8.657700E-10	2.088538E+15	6.363409E-01	0.000000E+00	3.875555E-04	0.000000E+00	3.632716E-01
1.084400E-09	1.985271E+15	5.796059E-01	0.000000E+00	3.493803E-04	0.000000E+00	4.200447E-01
1.974900E-09	1.195204E+15	9.780002E-01	0.000000E+00	1.580022E-04	0.000000E+00	2.184178E-02
Time (s)	$<\Theta_{tot}>$	$<f\_\Theta_{collBB}>$	$<f\_\Theta_{photoBB}>$	$<f\_\Theta_{collBF}>$	$<f\_\Theta_{photoBF}>$	$<f\_\Theta_{auto}>$
5.313700E-10	7.580161E+17	6.852151E-06	0.000000E+00	4.580480E-11	0.000000E+00	9.999931E-01
8.657700E-10	4.007531E+11	4.092422E-02	0.000000E+00	3.638107E-06	0.000000E+00	9.590721E-01
1.084400E-09	5.692786E+10	1.227187E-01	0.000000E+00	1.853032E-05	0.000000E+00	8.772627E-01
1.974900E-09	4.748621E+08	9.225390E-01	0.000000E+00	4.384346E-03	0.000000E+00	7.307664E-02
Time (s)	**<occ1>**	**<occ2>**	**<occ3>**	**<occ4>**	**<occ5>**	**<occ6>**
5.313700E-10	1.996503	6.254325	0.028598	0.005022	0.001271	0.000041
8.657700E-10	1.983917	0.004229	0.000404	0.000330	0.000148	0.000007
1.084400E-09	1.890732	0.001118	0.000200	0.000176	0.000081	0.000004
1.974900E-09	1.881834	0.000010	0.000012	0.000012	0.000006	0.000000

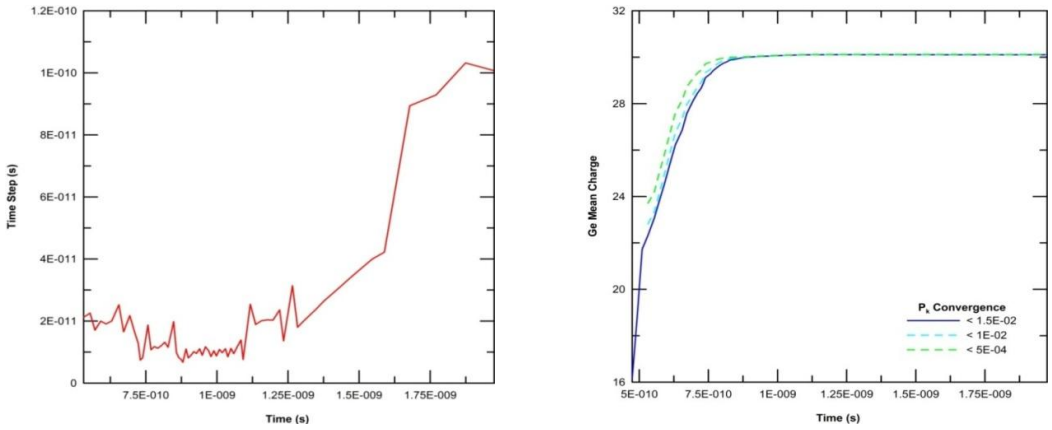

Fig. 7.b. Time step evolution of plasma case TD-Ge provided by workshop NLTE-3 (left). Temporal mean charge of germanium plasma computed with ATMED CR (right), with criteria of convergence in populations of < 1E-02, < 1.5E-02 or more strict < 5E-04

3. SUMMARY AND CONCLUSIONS

In this paper, there are modeled with ATMED CR plasmas proposed in the 3rd Non-LTE Code Comparison Workshop held in December 2003. Cases for C, Al, Ar, Ge, Xe and Au plasmas were selected for detailed comparisons. It has been observed a good agreement of atomic and radiative properties with respect to results of other codes which have participated in the storage inside the 3rd NLTE database [18-19]. A very complete description of the code ATMED CR can be found in both books of the doctoral thesis [2,24].

ACKNOWLEDGEMENTS

This work has been partially supported by a Research Project of the Spanish Ministry of Science and Innovation (ENE2009-11208), by a Research Project of the "Agencia Canaria de Investigación, Innovación y Sociedad de la Información" of the regional government of the Canary Islands (SOLSUBC2008000057) and also by the "Keep-in Touch" project of the European Union. The authors thankfully acknowledge the computer resources from Atlante, technical expertise and assistance provided by the Spanish SupercomputingNetwork (RES) and Instituto Tecnológico de Canarias Gobierno de Canarias.

COMPETING INTERESTS

Author has declared that no competing interests exist.

REFERENCES

1. Benita AJ, Mínguez E, Mendoza MA, Rubiano JG, Gil JM, Rodríguez R, Martel P. Collisional radiative average atom code based on a relativistic screened hydrogenic model. High Energy Density Physics. 2015;14:18-29.
2. Benita AJ. Collisional radiative average atom code with relativistic atomic model. Theoretical physics. LAP Lambert Academic Publishing; 2017. [ISBN: 978-620-2-01943-9].
3. Benita AJ. Fast calculation of plasmas properties with ATMED LTE. Project of Nuclear Science and Technology Master at UPM; 2012.
4. Mendoza MA, Rubiano JG, Gil JM, Rodriguez R, Florido R, Benita AJ, Martel P, Minguez E. Fast computation of radiative properties and EOS of warm dense matter using the ATMED code. Eight International Conference on Inertial Fusion Sciences and Applications (IFSA 2013). September 8-13 Nara, Japan; 2013.
5. Mendoza MA, Rubiano JG, Gil JM, Rodriguez R, Florido R, Espinosa G, Martel P, Minguez E. Calculation of radiative opacity of plasma mixtures using a relativistic screened hydrogenic model. Journal of Quantitative Spectroscopy & Radiative Transfer. 2014;140:81–98.
6. Mendoza MA, Rubiano JG, Gil JM, Rodriguez R, Florido R, Martel P, Minguez E. A new set of relativistic screening constants for the screened hydrogenic model. HEDP. 2011;7:169–179.

7. Ruano FH, Rubiano JG, Mendoza MA, Gil JM, Rodriguez R, Florido R, Martel P, Minguez E. Relativistic screened hydrogenic radial integrals. Journal of Quantitative Spectroscopy & Radiative Transfer. 2012;117:123-132.
8. Lokke WA, Grasberger WH. XSNQ-U A Non-LTE emission and absorption coefficient subroutine. Prepared for U.S. Energy Research & Development Administration under contract No. W-7405-Eng-48, UCRL-52276; 1977.
9. Joseph Abdallah et al. The reduced detailed configuration accounting (RDCA) model for NLTE plasma calculations. High Energy Density Physics. 2008;4:124–130.
10. Faussurier G, Blancard C, Kato T, More RM. Prigogine theorem of minimum entropy production applied to the average atom model. High Energy Density Physics. 2009;5:283–293.
11. Faussurier G, et al. Nonlocal thermodynamic equilibrium self-consistent average-atom model for plasma physics. Physical Review. 2001;63:026401.
12. Balazs F. Rozsnyai. Collisional radiative average atom model for hot plasmas. Physical Review E. 1996;55.
13. Balazs F. Rozsnyai. Hot plasma opacities in the presence or absence of local thermodynamic equilibrium. High Energy Density Physics. 2010;6:345–355.
14. Nikiforov AF, Novikov VG, Uvarov VB. Quantum-statistical models of hot dense matter. Methods for Computation Opacity and Equation of State. Birkhäuser Verlag; 2005.
15. Benita AJ. Calculation of temporal plasmas of XFEL experiments with a relativistic collisional radiative average atom code. Physical Science International Journal; 2018.
DOI: 10.9734/PSIJ/2018/40246
16. Benita AJ. Book Summary; 2017.
[ISBN 978-620-2-01943-9]
Available:https://www.researchgate.net/profile/Aj_Benita
17. Benita AJ. Comparison of iron plasma atomic and radiative properties computed with a relativistic collisional radiative average atom code versus other models. Asian Journal of Research and Reviews in Physics ; 2018.
DOI: 10.9734/AJR2P/2018/41729
18. Available:https://nlte.nist.gov/SAHA/
19. The Third Non-LTE Kinetics Workshop. Submission of Calculations. December 1-5, 2003. NIST, Gaithersburg MD.
20. Plasmas Computed with ATMED CR of the 4th Non-LTE Code Comparison Workshop Database. Physical Science International Journal. 2018;20(1):1-26.
[Article no.PSIJ.44683]
[ISSN: 2348-0130]
DOI: 10.9734/PSIJ/2018/44683
21. Florido R, et al. Modeling of population kinetics of plasmas that are not in local thermodynamic equilibrium, using a versatile collisional-radiative model based on analytical rates. Physical Review E. 2009;80:056402.
DOI: 10.1103/PhysRevE.80.056402
22. Chung HK, et al. FLYCHK: Generalized population kinetics and spectral model for rapid spectroscopic analysis for all elements. UCRL-JRNL-213347. High Energy Density Physics; 2005.
23. Scott HA, Hansen SB. Advances in NLTE modeling for integrated simulations. High Energy Density Physics. 2010;6:39–47.
Benita AJ. Set of plasmas with relativistic collisional radiative code ATMED CR. Physics, astronomy. LAP Lambert Academic Publishing; 2019.
[ISBN: 978-613-9-94744-7]

APPENDIX I

Table 1.a. Rates of collisional ionization for argon plasma at N_e = 1E+23 cm^{-3} and electronic temperature 100 eV of thermal electrons or hot very energetic electrons acting fundamentally stripping also the inner shells

Orbital number P_k	Energy Dirac's Eigenvalue (eV) P_k	T_e=100 eV & 10% Hot e- collisional ionization by thermal electrons (s^{-1})	T_e=100 eV & 10% Hot e- collisional ionization by hot electrons (s^{-1})	Energy Dirac's eigenvalue (eV) P_k	T_e=100 eV & 75% Hot e- collisional ionization by thermal electrons (s^{-1})	T_e=100 eV & 75% Hot e- collisional ionization by hot electrons (s^{-1})
1	**-3387.214559**	1.452343E-04	6.889573E+10	**-3783.442668**	4.623129E-07	4.136981E+11
2	**-509.596992**	4.478391E+10	1.397855E+12	**-776.940092**	4.357004E+08	5.909336E+12
3	**-433.793988**	1.247401E+11	1.725071E+12	**-732.092880**	7.672393E+08	6.440668E+12
4	**-417.531645**	1.316384E+11	1.745271E+12	**-724.816178**	7.954333E+08	6.476924E+12
5	**-136.440188**	2.421375E+13	8.236837E+12	**-299.218385**	3.307936E+11	2.237066E+13
6	**-120.379319**	3.521198E+13	9.641412E+12	**-291.542016**	3.742339E+11	2.315154E+13
7	**-118.034551**	3.688304E+13	9.836971E+12	**-289.890496**	3.833677E+11	2.330869E+13
8	**-92.706748**	7.139739E+13	1.328933E+13	**-276.198920**	4.793176E+11	2.483953E+13
9	**-92.091466**	7.235780E+13	1.337438E+13	**-275.365640**	4.854213E+11	2.493050E+13
10	**-54.375298**	2.544854E+14	2.578417E+13	**-154.807497**	4.529576E+12	5.267412E+13
11	**-46.605854**	3.510173E+14	3.106640E+13	**-150.563341**	4.958208E+12	5.456516E+13
12	**-46.497884**	3.513571E+14	3.108419E+13	**-150.120019**	5.000508E+12	5.474753E+13
13	**-38.823665**	5.027129E+14	3.860644E+13	**-145.606880**	5.513574E+12	5.690498E+13
14	**-37.746640**	5.299658E+14	3.989177E+13	**-144.880239**	5.599950E+12	5.725889E+13
15	**-36.399666**	5.676275E+14	4.164039E+13	**-143.549745**	5.763456E+12	5.792200E+13
16	**-35.431869**	5.969133E+14	4.297977E+13	**-142.901602**	5.845657E+12	5.825210E+13
17	**-25.993852**	1.060459E+15	6.252863E+13	**-91.969618**	2.059677E+13	1.013250E+14
18	**-23.842345**	1.232011E+15	6.922630E+13	**-90.541156**	2.144136E+13	1.033030E+14
19	**-22.269057**	1.381153E+15	7.488820E+13	**-89.638979**	2.198176E+13	1.045532E+14
20	**-17.429859**	2.076856E+15	9.988413E+13	**-87.093281**	2.365437E+13	1.083518E+14
21	**-17.415639**	2.077369E+15	9.990187E+13	**-87.052352**	2.367635E+13	1.084010E+14
22	**-15.610978**	2.473791E+15	1.133991E+14	**-85.670692**	2.464069E+13	1.105449E+14
23	**-15.603954**	2.473976E+15	1.134053E+14	**-85.650458**	2.465197E+13	1.105698E+14
24	**-14.905633**	2.655709E+15	1.194584E+14	**-85.049041**	2.507976E+13	1.115108E+14
25	**-14.901149**	2.655745E+15	1.194595E+14	**-85.036602**	2.508703E+13	1.115268E+14
26	**-10.598158**	4.535847E+15	1.787092E+14	**-59.237769**	5.868752E+13	1.739827E+14
27	**-10.145200**	4.839685E+15	1.878627E+14	**-58.873539**	5.948017E+13	1.752817E+14
28	**-10.122429**	4.841488E+15	1.879167E+14	**-58.808372**	5.958536E+13	1.754537E+14
29	**-9.172598**	5.606719E+15	2.105951E+14	**-57.964241**	6.150784E+13	1.785806E+14

30	**-9.166114**	5.607274E+15	2.106113E+14	**-57.943894**	6.154254E+13	1.786368E+14
31	**-8.493816**	6.266517E+15	2.297792E+14	**-57.291761**	6.307033E+13	1.810997E+14
32	**-8.490667**	6.266735E+15	2.297855E+14	**-57.281796**	6.308769E+13	1.811275E+14
33	**-8.220628**	6.562741E+15	2.382953E+14	**-57.017684**	6.371075E+13	1.821266E+14
34	**-8.218669**	6.562816E+15	2.382974E+14	**-57.011654**	6.372139E+13	1.821436E+14
35	**-7.665549**	7.247775E+15	2.577846E+14	**-56.434284**	6.511893E+13	1.843735E+14
36	**-7.664157**	7.247755E+15	2.577840E+14	**-56.430185**	6.512641E+13	1.843854E+14

Table 1.b. Rates of collisional ionization for argon plasma at N_e = 1E+23 cm^{-3} and electronic temperature 600 eV of thermal electrons or hot very energetic electrons acting fundamentally stripping also the inner shells

Orbital number P_k	Energy Dirac's Eigenvalue (eV) P_k	T_e=600 eV & 10% Hot e- collisional ionization by thermal electrons (s^{-1})	T_e=600 eV & 10% Hot e- collisional ionization by hot electrons (s^{-1})	Energy Dirac's Eigenvalue (eV) P_k	T_e=600 eV & 75% Hot e- collisional ionization by thermal electrons (s^{-1})	T_e=600 eV & 75% Hot e- collisional ionization by hot electrons (s^{-1})
1	**-3997.580902**	3.508223E+08	4.964852E+10	**-4223.168972**	7.158341E+07	3.532426E+11
2	**-920.829196**	1.142000E+12	6.212559E+11	**-1018.762293**	2.308219E+11	4.092006E+12
3	**-890.990783**	1.270455E+12	6.521826E+11	**-1003.699841**	2.429120E+11	4.184265E+12
4	**-885.996058**	1.292825E+12	6.574298E+11	**-998.847281**	2.469268E+11	4.214446E+12
5	**-393.110685**	1.147981E+13	2.069401E+12	**-444.423537**	2.447257E+12	1.340177E+13
6	**-391.563378**	1.158282E+13	2.080458E+12	**-443.717316**	2.456492E+12	1.343091E+13
7	**-390.457756**	1.165585E+13	2.088280E+12	**-442.464614**	2.472917E+12	1.348267E+13
8	**-385.816104**	1.197496E+13	2.122296E+12	**-440.250235**	2.502431E+12	1.357541E+13
9	**-385.155930**	1.202067E+13	2.127147E+12	**-439.686029**	2.509994E+12	1.359912E+13
10	**-218.369740**	3.890535E+13	4.513510E+12	**-248.513031**	8.584576E+12	2.918723E+13
11	**-217.367159**	3.924729E+13	4.540524E+12	**-248.042301**	8.616680E+12	2.925969E+13
12	**-216.890577**	3.940861E+13	4.553250E+12	**-247.506904**	8.653174E+12	2.934198E+13
13	**-215.563898**	3.987033E+13	4.589615E+12	**-246.882334**	8.696285E+12	2.943910E+13
14	**-215.199584**	3.999736E+13	4.599604E+12	**-246.604705**	8.715455E+12	2.948225E+13
15	**-214.755517**	4.015354E+13	4.611875E+12	**-246.394552**	8.729996E+12	2.951496E+13
16	**-214.445056**	4.026323E+13	4.620487E+12	**-246.193301**	8.743984E+12	2.954642E+13
17	**-137.993993**	8.911040E+13	8.128096E+12	**-158.105073**	1.993844E+13	5.234920E+13
18	**-137.095341**	9.011331E+13	8.195480E+12	**-157.663720**	2.003696E+13	5.253583E+13
19	**-136.736370**	9.051318E+13	8.222310E+12	**-157.338025**	2.010958E+13	5.267330E+13
20	**-136.433842**	9.085739E+13	8.245389E+12	**-157.211897**	2.013807E+13	5.272720E+13
21	**-136.369269**	9.092906E+13	8.250192E+12	**-157.129013**	2.015660E+13	5.276225E+13
22	**-136.125003**	9.120548E+13	8.268712E+12	**-157.014591**	2.018219E+13	5.281065E+13
23	**-136.092867**	9.124118E+13	8.271103E+12	**-156.973278**	2.019144E+13	5.282813E+13

24	**-135.974962**	9.137310E+13	8.279938E+12	**-156.911696**	2.020505E+13	5.285386E+13
25	**-135.955665**	9.139449E+13	8.281370E+12	**-156.886915**	2.021059E+13	5.286434E+13
26	**-94.591779**	1.665275E+14	1.304770E+13	**-109.178276**	3.742357E+13	8.353471E+13
27	**-94.522450**	1.667212E+14	1.305948E+13	**-109.142145**	3.744370E+13	8.356895E+13
28	**-94.411318**	1.670250E+14	1.307794E+13	**-108.998283**	3.752368E+13	8.370496E+13
29	**-94.247933**	1.674906E+14	1.310622E+13	**-108.913481**	3.757184E+13	8.378683E+13
30	**-94.211417**	1.675912E+14	1.311234E+13	**-108.866013**	3.759836E+13	8.383190E+13
31	**-94.081068**	1.679607E+14	1.313478E+13	**-108.797393**	3.763704E+13	8.389763E+13
32	**-94.062909**	1.680108E+14	1.313782E+13	**-108.773744**	3.765027E+13	8.392012E+13
33	**-94.005267**	1.681723E+14	1.314762E+13	**-108.742307**	3.766776E+13	8.394984E+13
34	**-93.994380**	1.682023E+14	1.314944E+13	**-108.728131**	3.767569E+13	8.396331E+13
35	**-93.871864**	1.685475E+14	1.317039E+13	**-108.661169**	3.771312E+13	8.402690E+13
36	**-93.864602**	1.685675E+14	1.317161E+13	**-108.651721**	3.771840E+13	8.403588E+13

Table 1.c. Rates of collisional excitation for argon plasma at N_e = 1E+23 cm^{-3} and electronic temperature 100 or 600 eV of thermal electrons or hot very energetic electrons acting fundamentally stripping also the inner shells

% Hot electrons	Orbital number P_k	Collisional excitation by 100 eV thermal electrons (s^{-1})	Collisional excitation by 10000 eV Hot electrons (s^{-1})	% Hot electrons	Orbital number P_k	Collisional excitation by 600 eV thermal electrons (s^{-1})	Collisional excitation by 10000 eV hot electrons (s^{-1})
10%	**1 → 6**	2.815531E-03	2.974310E+10	**10%**	**1 → 6**	1.953063E+09	4.484825E+10
	1 → 12	3.902917E-04	8.535124E+09		**1 → 12**	5.271129E+08	1.578110E+10
	1 → 18	1.185290E-04	3.241670E+09		**1 → 18**	2.171797E+08	7.340136E+09
	1 → 28	2.505801E-05	7.839699E+08		**1 → 28**	1.140055E+08	4.111240E+09
75%	**1 → 6**	9.469992E-05	3.231208E+11	**75%**	**1 → 6**	4.642157E+08	3.366533E+11
	1 → 12	8.399989E-06	1.149894E+11		**1 → 12**	1.186840E+08	1.159554E+11
	1 → 18	2.182190E-06	5.366048E+10		**1 → 18**	4.755530E+07	5.325879E+10
	1 → 28	8.532432E-07	2.864951E+10		**1 → 28**	2.467600E+07	2.975689E+10

APPENDIX II

Table 2.a. Evolution of germanium plasma parameters depending on the characteristics of the experiment with ATMED CR with criteria of convergence in populations of < 1E-02

Time (s)	T_e (eV)	N_e (cm^{-3})	ρ g/cm^3	Mean Charge Z_{bar}	N_{ion} ($ion.cm^{-3}$)	Time Step (s)
5.313700E-10	**200.250000**	2.424698E+20	0.001282	22.815345	1.062749E+19	2.123000E-11
5.539300E-10	**241.300000**	2.500567E+20	0.001293	23.326896	1.071967E+19	2.256000E-11
5.710200E-10	**274.370000**	2.546749E+20	0.001276	24.083975	1.057446E+19	1.709000E-11
5.910000E-10	**316.800000**	2.580686E+20	0.001246	24.976002	1.033266E+19	1.998000E-11
6.100800E-10	**359.320000**	2.586875E+20	0.001207	25.843447	1.000979E+19	1.908000E-11
6.301000E-10	**406.130000**	2.566818E+20	0.001158	26.735054	9.600946E+18	2.002000E-11
6.553400E-10	**467.340000**	2.526143E+20	0.001113	27.372312	9.228825E+18	2.524000E-11
6.718600E-10	**505.070000**	2.502619E+20	0.001079	27.966913	8.948499E+18	1.652000E-11
6.936300E-10	**560.720000**	2.485272E+20	0.001056	28.383184	8.756144E+18	2.177000E-11
7.101700E-10	**606.760000**	2.479839E+20	0.001042	28.708959	8.637856E+18	1.654000E-11
7.230600E-10	**642.860000**	2.474014E+20	0.001032	28.903661	8.559518E+18	1.289000E-11
7.304800E-10	**663.730000**	2.467273E+20	0.001023	29.085627	8.482790E+18	7.420000E-12
7.386500E-10	**686.850000**	2.456407E+20	0.001010	29.336979	8.373075E+18	8.170000E-12
7.573800E-10	**740.030000**	2.406867E+20	0.000985	29.477481	8.165105E+18	1.873000E-11
7.681100E-10	**770.070000**	2.365830E+20	0.000964	29.600173	7.992621E+18	1.073000E-11
7.799100E-10	**802.460000**	2.314356E+20	0.000940	29.695725	7.793567E+18	1.180000E-11
7.911600E-10	**831.520000**	2.264476E+20	0.000917	29.774609	7.605392E+18	1.125000E-11
8.031600E-10	**861.980000**	2.215932E+20	0.000896	29.839629	7.426139E+18	1.200000E-11
8.163500E-10	**894.560000**	2.174250E+20	0.000878	29.886725	7.274968E+18	1.319000E-11
8.279100E-10	**919.150000**	2.150185E+20	0.000866	29.938795	7.181936E+18	1.156000E-11
8.477300E-10	**955.330000**	2.135551E+20	0.000860	29.962001	7.127530E+18	1.982000E-11
8.575400E-10	**971.750000**	2.137331E+20	0.000860	29.977996	7.129666E+18	9.810000E-12
8.657700E-10	**983.600000**	2.140821E+20	0.000861	29.989442	7.138584E+18	8.230000E-12
8.734400E-10	**993.690000**	2.144019E+20	0.000862	29.997001	7.147445E+18	7.670000E-12
8.801600E-10	**1001.700000**	2.145422E+20	0.000862	30.005788	7.150027E+18	6.720000E-12
8.911800E-10	**1013.200000**	2.143024E+20	0.000861	30.011562	7.140660E+18	1.102000E-11
8.993200E-10	**1020.600000**	2.136324E+20	0.000858	30.017511	7.116925E+18	8.140000E-12
9.082000E-10	**1027.400000**	2.123628E+20	0.000853	30.023931	7.073117E+18	8.880000E-12
9.183600E-10	**1033.900000**	2.102835E+20	0.000845	30.029715	7.002515E+18	1.016000E-11
9.279400E-10	**1038.700000**	2.078639E+20	0.000835	30.036117	6.920465E+18	9.580000E-12
9.390000E-10	**1043.100000**	2.048024E+20	0.000822	30.041364	6.817348E+18	1.106000E-11
9.479800E-10	**1045.500000**	2.023524E+20	0.000812	30.047902	6.734328E+18	8.980000E-12

9.596900E-10	**1047.100000**	1.994821E+20	0.000801	30.053532	6.637559E+18	1.171000E-11
9.701800E-10	**1047.200000**	1.972206E+20	0.000791	30.057847	6.561369E+18	1.049000E-11
9.787600E-10	**1046.500000**	1.959588E+20	0.000786	30.062807	6.518313E+18	8.580000E-12
9.892000E-10	**1045.300000**	1.948918E+20	0.000782	30.066872	6.481944E+18	1.044000E-11
9.979500E-10	**1043.300000**	1.943491E+20	0.000780	30.071552	6.462889E+18	8.750000E-12
1.008800E-09	**1039.900000**	1.939413E+20	0.000778	30.075616	6.448456E+18	1.085000E-11
1.018600E-09	**1035.700000**	1.936582E+20	0.000777	30.079900	6.438128E+18	9.800000E-12
1.029700E-09	**1030.200000**	1.932111E+20	0.000775	30.082981	6.422605E+18	1.110000E-11
1.038200E-09	**1025.800000**	1.926560E+20	0.000772	30.086685	6.403363E+18	8.500000E-12
1.049400E-09	**1019.700000**	1.914993E+20	0.000768	30.089606	6.364301E+18	1.120000E-11
1.058900E-09	**1014.000000**	1.899002E+20	0.000761	30.092921	6.310461E+18	9.500000E-12
1.070500E-09	**1006.300000**	1.877404E+20	0.000752	30.096437	6.237960E+18	1.160000E-11
1.084400E-09	**996.040000**	1.846700E+20	0.000740	30.098146	6.135595E+18	1.390000E-11
1.092000E-09	**989.940000**	1.829106E+20	0.000733	30.103068	6.076146E+18	7.600000E-12
1.117400E-09	**967.750000**	1.772702E+20	0.000710	30.105789	5.888242E+18	2.540000E-11
1.136300E-09	**949.800000**	1.738600E+20	0.000697	30.107968	5.774553E+18	1.890000E-11
1.156400E-09	**928.870000**	1.709800E+20	0.000685	30.109533	5.678601E+18	2.010000E-11
1.176800E-09	**906.070000**	1.684700E+20	0.000675	30.110548	5.595050E+18	2.040000E-11
1.197100E-09	**881.970000**	1.659100E+20	0.000665	30.111219	5.509906E+18	2.030000E-11
1.220700E-09	**853.820000**	1.624200E+20	0.000651	30.111403	5.393970E+18	2.360000E-11
1.234300E-09	**837.200000**	1.601300E+20	0.000641	30.111473	5.317908E+18	1.360000E-11
1.265700E-09	**799.130000**	1.544300E+20	0.000619	30.111384	5.128626E+18	3.140000E-11
1.283700E-09	**776.940000**	1.512300E+20	0.000606	30.111195	5.022385E+18	1.800000E-11
1.303600E-09	**752.750000**	1.480300E+20	0.000593	30.110953	4.916151E+18	1.990000E-11
1.325400E-09	**726.670000**	1.449600E+20	0.000581	30.110677	4.814240E+18	2.180000E-11
1.349300E-09	**698.780000**	1.420300E+20	0.000569	30.110394	4.716976E+18	2.390000E-11
1.375700E-09	**669.690000**	1.390600E+20	0.000557	30.110122	4.618381E+18	2.640000E-11
1.404400E-09	**639.490000**	1.357800E+20	0.000544	30.109875	4.509484E+18	2.870000E-11
1.435600E-09	**608.890000**	1.319400E+20	0.000529	30.109652	4.381984E+18	3.120000E-11
1.469600E-09	**578.210000**	1.274500E+20	0.000511	30.109458	4.232890E+18	3.400000E-11
1.506500E-09	**548.070000**	1.225000E+20	0.000491	30.109282	4.068513E+18	3.690000E-11
1.546500E-09	**518.510000**	1.175400E+20	0.000471	30.109122	3.903801E+18	4.000000E-11
1.588700E-09	**492.100000**	1.131400E+20	0.000453	30.108805	3.757706E+18	4.220000E-11
1.678100E-09	**442.950000**	1.095200E+20	0.000439	30.108488	3.637514E+18	8.940000E-11
1.771000E-09	**403.690000**	1.163200E+20	0.000466	30.108065	3.863418E+18	9.290000E-11
1.874200E-09	**369.570000**	1.256901E+20	0.000504	30.107543	4.174704E+18	1.032000E-10
1.974900E-09	**342.400000**	1.252603E+20	0.000502	30.107030	4.160501E+18	1.007000E-10

Table 2.b. Evolution of germanium plasma parameters depending on the characteristics of the experiment with ATMED CR with criteria of convergence in populations of < 5E-04

Time (s)	T_e (eV)	N_e (cm^{-3})	ρ g/cm^3	Mean Charge Z_{bar}	N_{ion} ($ion.cm^{-3}$)	Time Step (s)
5.313700E-10	**200.250000**	2.422726E+20	0.001232	23.714239	1.021633E+19	2.123000E-11
5.539300E-10	**241.300000**	2.496754E+20	0.001246	24.178202	1.032647E+19	2.256000E-11
5.710200E-10	**274.370000**	2.546099E+20	0.001230	24.964815	1.019875E+19	1.709000E-11
5.910000E-10	**316.800000**	2.579934E+20	0.001205	25.824079	9.990419E+18	1.998000E-11
6.100800E-10	**359.320000**	2.586083E+20	0.001169	26.683918	9.691543E+18	1.908000E-11
6.301000E-10	**406.130000**	2.565904E+20	0.001122	27.587440	9.300986E+18	2.002000E-11
6.553400E-10	**467.340000**	2.522420E+20	0.001080	28.165787	8.955617E+18	2.524000E-11
6.718600E-10	**505.070000**	2.499231E+20	0.001049	28.724982	8.700550E+18	1.652000E-11
6.936300E-10	**560.720000**	2.482840E+20	0.001030	29.083775	8.536857E+18	2.177000E-11
7.101700E-10	**606.760000**	2.478182E+20	0.001020	29.317684	8.452858E+18	1.654000E-11
7.230600E-10	**642.860000**	2.472922E+20	0.001013	29.438835	8.400204E+18	1.289000E-11
7.304800E-10	**663.730000**	2.466318E+20	0.001007	29.549419	8.346418E+18	7.420000E-12
7.386500E-10	**686.850000**	2.454504E+20	0.000996	29.713572	8.260548E+18	8.170000E-12
7.573800E-10	**740.030000**	2.405568E+20	0.000974	29.790111	8.075055E+18	1.873000E-11
7.681100E-10	**770.070000**	2.364874E+20	0.000956	29.852323	7.921911E+18	1.073000E-11
7.799100E-10	**802.460000**	2.313686E+20	0.000933	29.896769	7.738915E+18	1.180000E-11
7.911600E-10	**831.520000**	2.263989E+20	0.000912	29.931332	7.563943E+18	1.125000E-11
8.031600E-10	**861.980000**	2.215694E+20	0.000892	29.958464	7.395886E+18	1.200000E-11
8.163500E-10	**894.560000**	2.174097E+20	0.000875	29.976484	7.252675E+18	1.319000E-11
8.279100E-10	**919.150000**	2.150098E+20	0.000865	29.994288	7.168358E+18	1.156000E-11
8.477300E-10	**955.330000**	2.135499E+20	0.000859	30.001290	7.118024E+18	1.982000E-11
8.575400E-10	**971.750000**	2.137299E+20	0.000859	30.006430	7.122803E+18	9.810000E-12
8.657700E-10	**983.600000**	2.140799E+20	0.000860	30.010966	7.133390E+18	8.230000E-12
8.734400E-10	**993.690000**	2.143999E+20	0.000862	30.014897	7.143116E+18	7.670000E-12
8.801600E-10	**1001.700000**	2.145399E+20	0.000862	30.021080	7.146309E+18	6.720000E-12
8.911800E-10	**1013.200000**	2.142999E+20	0.000861	30.025751	7.137203E+18	1.102000E-11
8.993200E-10	**1020.600000**	2.136297E+20	0.000858	30.030844	7.113678E+18	8.140000E-12
9.082000E-10	**1027.400000**	2.123597E+20	0.000853	30.036609	7.070030E+18	8.880000E-12
9.183600E-10	**1033.900000**	2.102797E+20	0.000844	30.042014	6.999521E+18	1.016000E-11
9.279400E-10	**1038.700000**	2.078598E+20	0.000834	30.048128	6.917563E+18	9.580000E-12
9.390000E-10	**1043.100000**	2.047998E+20	0.000822	30.053021	6.814617E+18	1.106000E-11
9.479800E-10	**1045.500000**	2.023497E+20	0.000812	30.059165	6.731716E+18	8.980000E-12
9.596900E-10	**1047.100000**	1.994798E+20	0.000800	30.064470	6.635067E+18	1.171000E-11
9.701800E-10	**1047.200000**	1.973898E+20	0.000792	30.068652	6.564639E+18	1.049000E-11

9.787600E-10	**1046.500000**	1.960998E+20	0.000787	30.073508	6.520683E+18	8.580000E-12
9.892000E-10	**1045.300000**	1.949999E+20	0.000782	30.077414	6.483265E+18	1.044000E-11
9.979500E-10	**1043.300000**	1.944198E+20	0.000780	30.082011	6.462992E+18	8.750000E-12
1.008800E-09	**1039.900000**	1.939598E+20	0.000778	30.085929	6.446862E+18	1.085000E-11
1.018600E-09	**1035.700000**	1.936298E+20	0.000776	30.090073	6.435006E+18	9.800000E-12
1.029700E-09	**1030.200000**	1.931299E+20	0.000774	30.093028	6.417762E+18	1.110000E-11
1.038200E-09	**1025.800000**	1.931298E+20	0.000774	30.096655	6.416987E+18	8.500000E-12
1.049400E-09	**1019.700000**	1.913199E+20	0.000767	30.099486	6.356251E+18	1.120000E-11
1.058900E-09	**1014.000000**	1.898999E+20	0.000761	30.102652	6.308410E+18	9.500000E-12
1.070500E-09	**1006.300000**	1.877399E+20	0.000752	30.106048	6.235952E+18	1.160000E-11
1.084400E-09	**996.040000**	1.846700E+20	0.000740	30.107688	6.133648E+18	1.390000E-11
1.092000E-09	**989.940000**	1.829098E+20	0.000733	30.112502	6.074213E+18	7.600000E-12
1.117400E-09	**967.750000**	1.772699E+20	0.000710	30.115168	5.886399E+18	2.540000E-11
1.136300E-09	**949.800000**	1.738599E+20	0.000696	30.117310	5.772757E+18	1.890000E-11
1.156400E-09	**928.870000**	1.709800E+20	0.000685	30.118866	5.676839E+18	2.010000E-11
1.176800E-09	**906.070000**	1.684700E+20	0.000675	30.119890	5.593313E+18	2.040000E-11
1.197100E-09	**881.970000**	1.659100E+20	0.000664	30.120586	5.508192E+18	2.030000E-11
1.220700E-09	**853.820000**	1.624200E+20	0.000650	30.120787	5.392290E+18	2.360000E-11
1.234300E-09	**837.200000**	1.601300E+20	0.000641	30.120926	5.316238E+18	1.360000E-11
1.265700E-09	**799.130000**	1.544300E+20	0.000618	30.120876	5.127010E+18	3.140000E-11
1.283700E-09	**776.940000**	1.512300E+20	0.000606	30.120727	5.020796E+18	1.800000E-11
1.303600E-09	**752.750000**	1.480300E+20	0.000593	30.120530	4.914589E+18	1.990000E-11
1.325400E-09	**726.670000**	1.449600E+20	0.000581	30.120307	4.812701E+18	2.180000E-11
1.349300E-09	**698.780000**	1.420300E+20	0.000569	30.120076	4.715461E+18	2.390000E-11
1.375700E-09	**669.690000**	1.390601E+20	0.000557	30.119859	4.616889E+18	2.640000E-11
1.404400E-09	**639.490000**	1.357801E+20	0.000544	30.119667	4.508020E+18	2.870000E-11
1.435600E-09	**608.890000**	1.319401E+20	0.000528	30.119506	4.380552E+18	3.120000E-11
1.469600E-09	**578.210000**	1.274501E+20	0.000510	30.119374	4.231497E+18	3.400000E-11
1.506500E-09	**548.070000**	1.225001E+20	0.000491	30.119266	4.067166E+18	3.690000E-11
1.546500E-09	**518.510000**	1.175401E+20	0.000471	30.119178	3.902499E+18	4.000000E-11
1.588700E-09	**492.100000**	1.131401E+20	0.000453	30.119016	3.756435E+18	4.220000E-11
1.678100E-09	**442.950000**	1.095202E+20	0.000439	30.118866	3.636264E+18	8.940000E-11
1.771000E-09	**403.690000**	1.163203E+20	0.000466	30.118662	3.862067E+18	9.290000E-11
1.874200E-09	**369.570000**	1.256905E+20	0.000503	30.118405	4.173213E+18	1.032000E-10
1.974900E-09	**342.400000**	1.252607E+20	0.000502	30.118126	4.158979E+18	1.007000E-10

Table 2.c. Evolution of germanium plasma parameters depending on the characteristics of the experiment with ATMED CR with criteria of convergence in populations of < 1.5E-02

Time (s)	T_e (eV)	N_e (cm^{-3})	ρ g/cm^3	Mean Charge Z_{bar}	N_{ion} ($ion.cm^{-3}$)	Time Step (s)
4.744100E-10	**82.758000**	2.283244E+20	0.001703	16.170714	1.411963E+19	2.230000E-11
4.921400E-10	**133.840000**	2.312206E+20	0.001484	18.790126	1.230543E+19	1.773000E-11
5.101400E-10	**170.850000**	2.350270E+20	0.001305	21.723998	1.081877E+19	1.800000E-11
5.313700E-10	**200.250000**	2.423240E+20	0.001309	22.328862	1.085250E+19	2.123000E-11
5.539300E-10	**241.300000**	2.499372E+20	0.001307	23.059150	1.083896E+19	2.256000E-11
5.710200E-10	**274.370000**	2.547325E+20	0.001293	23.755102	1.072328E+19	1.709000E-11
5.910000E-10	**316.800000**	2.581318E+20	0.001269	24.544956	1.051669E+19	1.998000E-11
6.100800E-10	**359.320000**	2.587698E+20	0.001230	25.385865	1.019346E+19	1.908000E-11
6.301000E-10	**406.130000**	2.567736E+20	0.001181	26.221463	9.792499E+18	2.002000E-11
6.553400E-10	**467.340000**	2.525677E+20	0.001134	26.868711	9.400069E+18	2.524000E-11
6.718600E-10	**505.070000**	2.501796E+20	0.001094	27.579103	9.071346E+18	1.652000E-11
6.936300E-10	**560.720000**	2.485748E+20	0.001067	28.109059	8.843226E+18	2.177000E-11
7.101700E-10	**606.760000**	2.480788E+20	0.001052	28.451266	8.719428E+18	1.654000E-11
7.230600E-10	**642.860000**	2.474916E+20	0.001042	28.653701	8.637334E+18	1.289000E-11
7.304800E-10	**663.730000**	2.468182E+20	0.001032	28.841829	8.557647E+18	7.420000E-12
7.386500E-10	**686.850000**	2.456275E+20	0.001018	29.113792	8.436809E+18	8.170000E-12
7.573800E-10	**740.030000**	2.406714E+20	0.000991	29.287564	8.217527E+18	1.873000E-11
7.681100E-10	**770.070000**	2.366853E+20	0.000970	29.431113	8.042010E+18	1.073000E-11
7.799100E-10	**802.460000**	2.315215E+20	0.000945	29.546278	7.835894E+18	1.180000E-11
7.911600E-10	**831.520000**	2.265087E+20	0.000922	29.649029	7.639666E+18	1.125000E-11
8.031600E-10	**861.980000**	2.216259E+20	0.000899	29.735958	7.453130E+18	1.200000E-11
8.163500E-10	**894.560000**	2.174498E+20	0.000880	29.801156	7.296688E+18	1.319000E-11
8.279100E-10	**919.150000**	2.150358E+20	0.000868	29.876463	7.197498E+18	1.156000E-11
8.477300E-10	**955.330000**	2.135667E+20	0.000861	29.912544	7.139704E+18	1.982000E-11
8.575400E-10	**971.750000**	2.137421E+20	0.000861	29.938573	7.139355E+18	9.810000E-12
8.657700E-10	**983.600000**	2.140883E+20	0.000862	29.959216	7.145990E+18	8.230000E-12
8.734400E-10	**993.690000**	2.144062E+20	0.000863	29.974101	7.153050E+18	7.670000E-12
8.801600E-10	**1001.700000**	2.145440E+20	0.000863	29.990557	7.153720E+18	6.720000E-12
8.911800E-10	**1013.200000**	2.143034E+20	0.000862	29.999613	7.143538E+18	1.102000E-11
8.993200E-10	**1020.600000**	2.136341E+20	0.000859	30.007142	7.119440E+18	8.140000E-12
9.082000E-10	**1027.400000**	2.123652E+20	0.000853	30.014430	7.075437E+18	8.880000E-12
9.183600E-10	**1033.900000**	2.102857E+20	0.000845	30.020856	7.004654E+18	1.016000E-11
9.279400E-10	**1038.700000**	2.078660E+20	0.000835	30.027898	6.922430E+18	9.580000E-12
9.390000E-10	**1043.100000**	2.048050E+20	0.000823	30.033566	6.819205E+18	1.106000E-11
9.479800E-10	**1045.500000**	2.023565E+20	0.000813	30.040400	6.736147E+18	8.980000E-12

9.596900E-10	**1047.100000**	1.994847E+20	0.000801	30.046447	6.639212E+18	1.171000E-11
9.701800E-10	**1047.200000**	1.973935E+20	0.000792	30.051244	6.568562E+18	1.049000E-11
9.787600E-10	**1046.500000**	1.961036E+20	0.000787	30.056780	6.524438E+18	8.580000E-12
9.892000E-10	**1045.300000**	1.950025E+20	0.000782	30.061244	6.486842E+18	1.044000E-11
9.979500E-10	**1043.300000**	1.944240E+20	0.000780	30.066369	6.466493E+18	8.750000E-12
1.008800E-09	**1039.900000**	1.939624E+20	0.000778	30.070799	6.450192E+18	1.085000E-11
1.018600E-09	**1035.700000**	1.936326E+20	0.000777	30.075448	6.438228E+18	9.800000E-12
1.029700E-09	**1030.200000**	1.931314E+20	0.000774	30.078770	6.420856E+18	1.110000E-11
1.038200E-09	**1025.800000**	1.925322E+20	0.000772	30.082795	6.400078E+18	8.500000E-12
1.049400E-09	**1019.700000**	1.913215E+20	0.000767	30.085936	6.359168E+18	1.120000E-11
1.058900E-09	**1014.000000**	1.899017E+20	0.000761	30.089439	6.311242E+18	9.500000E-12
1.070500E-09	**1006.300000**	1.877418E+20	0.000753	30.093175	6.238685E+18	1.160000E-11
1.084400E-09	**996.040000**	1.846706E+20	0.000740	30.094969	6.136263E+18	1.390000E-11
1.092000E-09	**989.940000**	1.829137E+20	0.000733	30.100097	6.076846E+18	7.600000E-12
1.117400E-09	**967.750000**	1.772712E+20	0.000710	30.102993	5.888824E+18	2.540000E-11
1.136300E-09	**949.800000**	1.738610E+20	0.000697	30.105289	5.775100E+18	1.890000E-11
1.156400E-09	**928.870000**	1.709808E+20	0.000685	30.106927	5.679118E+18	2.010000E-11
1.176800E-09	**906.070000**	1.683452E+20	0.000674	30.107918	5.591391E+18	2.040000E-11
1.197100E-09	**881.970000**	1.659906E+20	0.000665	30.108549	5.513071E+18	2.030000E-11
1.220700E-09	**853.820000**	1.624202E+20	0.000651	30.108738	5.394452E+18	2.360000E-11
1.234300E-09	**837.200000**	1.601304E+20	0.000642	30.108798	5.318392E+18	1.360000E-11
1.265700E-09	**799.130000**	1.544301E+20	0.000619	30.108703	5.129086E+18	3.140000E-11
1.283700E-09	**776.940000**	1.512301E+20	0.000606	30.108506	5.022836E+18	1.800000E-11
1.303600E-09	**752.750000**	1.480301E+20	0.000593	30.108240	4.916598E+18	1.990000E-11
1.325400E-09	**726.670000**	1.449601E+20	0.000581	30.107952	4.814678E+18	2.180000E-11
1.349300E-09	**698.780000**	1.420301E+20	0.000569	30.107646	4.717409E+18	2.390000E-11
1.375700E-09	**669.690000**	1.390601E+20	0.000557	30.107343	4.618809E+18	2.640000E-11
1.404400E-09	**639.490000**	1.357801E+20	0.000544	30.107062	4.509907E+18	2.870000E-11
1.435600E-09	**608.890000**	1.319401E+20	0.000529	30.106807	4.382400E+18	3.120000E-11
1.469600E-09	**578.210000**	1.274501E+20	0.000511	30.106574	4.233296E+18	3.400000E-11
1.506500E-09	**548.070000**	1.225000E+20	0.000491	30.106355	4.068910E+18	3.690000E-11
1.546500E-09	**518.510000**	1.175400E+20	0.000471	30.106148	3.904187E+18	4.000000E-11
1.588700E-09	**492.100000**	1.131401E+20	0.000453	30.105728	3.758092E+18	4.220000E-11
1.678100E-09	**442.950000**	1.095201E+20	0.000439	30.105315	3.637898E+18	8.940000E-11
1.771000E-09	**403.690000**	1.163201E+20	0.000466	30.104775	3.863842E+18	9.290000E-11
1.874200E-09	**369.570000**	1.256901E+20	0.000504	30.104111	4.175181E+18	1.032000E-10
1.974900E-09	**342.400000**	1.252601E+20	0.000502	30.103393	4.160997E+18	1.007000E-10

Table 2.d. Data for comparison of input density with the density ATMED CR computes for the iterative loop checking the coincidence up to the second decimal figure at least followed by power E+20, considering criteria for convergence in populations < 1E-02, < 1.5E-02 or more strict of < 5E-04

Step #	Time (s)	T_e	Input Data	of Grid N_e	P_k < 1E-02	ATMED CR N_e	P_k < 5E-04	ATMED CR N_e	P_k < 1.5E-02	ATMED CR N_e
11	4.7441E-10	8.2758E+01	**2.2823E+20**		-		-		2.283244E+20	
12	4.9214E-10	1.3384E+02	**2.3100E+20**		-		-		2.312206E+20	
13	5.1014E-10	1.7085E+02	**2.3522E+20**		-		-		2.350270E+20	
14	5.3137E-10	2.0025E+02	**2.4230E+20**		2.424698E+20		2.422726E+20		2.423240E+20	
15	5.5393E-10	2.4130E+02	**2.4981E+20**		2.500567E+20		2.496754E+20		2.499372E+20	
16	5.7102E-10	2.7437E+02	**2.5455E+20**		2.546749E+20		2.546099E+20		2.547325E+20	
17	5.9100E-10	3.1680E+02	**2.5793E+20**		2.580686E+20		2.579934E+20		2.581318E+20	
18	6.1008E-10	3.5932E+02	**2.5855E+20**		2.586875E+20		2.586083E+20		2.587698E+20	
19	6.3010E-10	4.0613E+02	**2.5655E+20**		2.566818E+20		2.565904E+20		2.567736E+20	
20	6.5534E-10	4.6734E+02	**2.5237E+20**		2.526143E+20		2.522420E+20		2.525677E+20	
21	6.7186E-10	5.0507E+02	**2.5003E+20**		2.502619E+20		2.499231E+20		2.501796E+20	
22	6.9363E-10	5.6072E+02	**2.4833E+20**		2.485272E+20		2.482840E+20		2.485748E+20	
23	7.1017E-10	6.0676E+02	**2.4784E+20**		2.479839E+20		2.478182E+20		2.480788E+20	
24	7.2306E-10	6.4286E+02	**2.4730E+20**		2.474014E+20		2.472922E+20		2.474916E+20	
25	7.3048E-10	6.6373E+02	**2.4664E+20**		2.467273E+20		2.466318E+20		2.468182E+20	
26	7.3865E-10	6.8685E+02	**2.4546E+20**		2.456407E+20		2.454504E+20		2.456275E+20	
27	7.5738E-10	7.4003E+02	**2.4056E+20**		2.406867E+20		2.405568E+20		2.406714E+20	
28	7.6811E-10	7.7007E+02	**2.3649E+20**		2.365830E+20		2.364874E+20		2.366853E+20	
29	7.7991E-10	8.0246E+02	**2.3137E+20**		2.314356E+20		2.313686E+20		2.315215E+20	
30	7.9116E-10	8.3152E+02	**2.2640E+20**		2.264476E+20		2.263989E+20		2.265087E+20	
31	8.0316E-10	8.6198E+02	**2.2157E+20**		2.215932E+20		2.215694E+20		2.216259E+20	
32	8.1635E-10	8.9456E+02	**2.1741E+20**		2.174250E+20		2.174097E+20		2.174498E+20	
33	8.2791E-10	9.1915E+02	**2.1501E+20**		2.150185E+20		2.150098E+20		2.150358E+20	
34	8.4773E-10	9.5533E+02	**2.1355E+20**		2.135551E+20		2.135499E+20		2.135667E+20	
35	8.5754E-10	9.7175E+02	**2.1373E+20**		2.137331E+20		2.137299E+20		2.137421E+20	
36	8.6577E-10	9.8360E+02	**2.1408E+20**		2.140821E+20		2.140799E+20		2.140883E+20	
37	8.7344E-10	9.9369E+02	**2.1440E+20**		2.144019E+20		2.143999E+20		2.144062E+20	
38	8.8016E-10	1.0017E+03	**2.1454E+20**		2.145422E+20		2.145399E+20		2.145440E+20	
39	8.9118E-10	1.0132E+03	**2.1430E+20**		2.143024E+20		2.142999E+20		2.143034E+20	
40	8.9932E-10	1.0206E+03	**2.1363E+20**		2.136324E+20		2.136297E+20		2.136341E+20	
41	9.0820E-10	1.0274E+03	**2.1236E+20**		2.123628E+20		2.123597E+20		2.123652E+20	

Step #	Time (s)	T_e	Input Data	of Grid N_e	P_k < 1E-02	ATMED CR N_e	P_k < 5E-04	ATMED CR N_e	P_k < 1.5E-02	ATMED CR N_e
42	9.1836E-10	1.0339E+03	**2.1028E+20**		2.102835E+20		2.102797E+20		2.102857E+20	
43	9.2794E-10	1.0387E+03	**2.0786E+20**		2.078639E+20		2.078598E+20		2.078660E+20	
44	9.3900E-10	1.0431E+03	**2.0480E+20**		2.048024E+20		2.047998E+20		2.048050E+20	
45	9.4798E-10	1.0455E+03	**2.0235E+20**		2.023524E+20		2.023497E+20		2.023565E+20	
46	9.5969E-10	1.0471E+03	**1.9948E+20**		1.994821E+20		1.994798E+20		1.994847E+20	
47	9.7018E-10	1.0472E+03	**1.9739E+20**		1.972206E+20		1.973898E+20		1.973935E+20	
48	9.7876E-10	1.0465E+03	**1.9610E+20**		1.959588E+20		1.960998E+20		1.961036E+20	
49	9.8920E-10	1.0453E+03	**1.9500E+20**		1.948918E+20		1.949999E+20		1.950025E+20	
50	9.9795E-10	1.0433E+03	**1.9442E+20**		1.943491E+20		1.944198E+20		1.944240E+20	
51	1.0088E-09	1.0399E+03	**1.9396E+20**		1.939413E+20		1.939598E+20		1.939624E+20	
52	1.0186E-09	1.0357E+03	**1.9363E+20**		1.936582E+20		1.936298E+20		1.936326E+20	
53	1.0297E-09	1.0302E+03	**1.9313E+20**		1.932111E+20		1.931299E+20		1.931314E+20	
54	1.0382E-09	1.0258E+03	**1.9253E+20**		1.926560E+20		1.931298E+20		1.925322E+20	
55	1.0494E-09	1.0197E+03	**1.9132E+20**		1.914993E+20		1.913199E+20		1.913215E+20	
56	1.0589E-09	1.0140E+03	**1.8990E+20**		1.899002E+20		1.898999E+20		1.899017E+20	
57	1.0705E-09	1.0063E+03	**1.8774E+20**		1.877404E+20		1.877399E+20		1.877418E+20	
58	1.0844E-09	9.9604E+02	**1.8467E+20**		1.846700E+20		1.846700E+20		1.846706E+20	
59	1.0920E-09	9.8994E+02	**1.8291E+20**		1.829106E+20		1.829098E+20		1.829137E+20	
60	1.1174E-09	9.6775E+02	**1.7727E+20**		1.772702E+20		1.772699E+20		1.772712E+20	
61	1.1363E-09	9.4980E+02	**1.7386E+20**		1.738600E+20		1.738599E+20		1.738610E+20	
62	1.1564E-09	9.2887E+02	**1.7098E+20**		1.709800E+20		1.709800E+20		1.709808E+20	
63	1.1768E-09	9.0607E+02	**1.6847E+20**		1.684700E+20		1.684700E+20		1.683452E+20	
64	1.1971E-09	8.8197E+02	**1.6591E+20**		1.659100E+20		1.659100E+20		1.659906E+20	
65	1.2207E-09	8.5382E+02	**1.6242E+20**		1.624200E+20		1.624200E+20		1.624202E+20	
66	1.2343E-09	8.3720E+02	**1.6013E+20**		1.601300E+20		1.601300E+20		1.601304E+20	
67	1.2657E-09	7.9913E+02	**1.5443E+20**		1.544300E+20		1.544300E+20		1.544301E+20	
68	1.2837E-09	7.7694E+02	**1.5123E+20**		1.512300E+20		1.512300E+20		1.512301E+20	
69	1.3036E-09	7.5275E+02	**1.4803E+20**		1.480300E+20		1.480300E+20		1.480301E+20	
70	1.3254E-09	7.2667E+02	**1.4496E+20**		1.449600E+20		1.449600E+20		1.449601E+20	
71	1.3493E-09	6.9878E+02	**1.4203E+20**		1.420300E+20		1.420300E+20		1.420301E+20	
72	1.3757E-09	6.6969E+02	**1.3906E+20**		1.390600E+20		1.390601E+20		1.390601E+20	
73	1.4044E-09	6.3949E+02	**1.3578E+20**		1.357800E+20		1.357801E+20		1.357801E+20	
74	1.4356E-09	6.0889E+02	**1.3194E+20**		1.319400E+20		1.319401E+20		1.319401E+20	
75	1.4696E-09	5.7821E+02	**1.2745E+20**		1.274500E+20		1.274501E+20		1.274501E+20	

Step #	Time (s)	T_e	Input Data	of Grid N_e	P_k < 1E-02	ATMED CR N_e	P_k < 5E-04	ATMED CR N_e	P_k < 1.5E-02	ATMED CR N_e
76	1.5065E-09	5.4807E+02	**1.2250E+20**		1.225000E+20		1.225001E+20		1.225000E+20	
77	1.5465E-09	5.1851E+02	**1.1754E+20**		1.175400E+20		1.175401E+20		1.175400E+20	
78	1.5887E-09	4.9210E+02	**1.1314E+20**		1.131400E+20		1.131401E+20		1.131401E+20	
79	1.6781E-09	4.4295E+02	**1.0952E+20**		1.095200E+20		1.095202E+20		1.095201E+20	
80	1.7710E-09	4.0369E+02	**1.1632E+20**		1.163200E+20		1.163203E+20		1.163201E+20	
81	1.8742E-09	3.6957E+02	**1.2569E+20**		1.256901E+20		1.256905E+20		1.256901E+20	
82	1.9749E-09	3.4240E+02	**1.2526E+20**		1.252603E+20		1.252607E+20		1.252601E+20	

Table 2.e. Evolution of germanium plasma fractional orbital populations in the average atom computed with ATMED CR with criteria of convergence in populations of < 1E-02

Time (s)	<occ1>	<occ2>	<occ3>	<occ4>	<occ5>	<occ6>
5.313700E-10	1.996457	7.135317	0.043153	0.007621	0.002039	0.000068
5.539300E-10	1.996447	6.626846	0.038425	0.008803	0.002494	0.000089
5.710200E-10	1.996463	5.876843	0.031700	0.008434	0.002494	0.000092
5.910000E-10	1.996490	4.989918	0.026538	0.008461	0.002495	0.000095
6.100800E-10	1.996527	4.127288	0.022358	0.007858	0.002427	0.000095
6.301000E-10	1.996575	3.240534	0.018425	0.007053	0.002269	0.000091
6.553400E-10	1.996619	2.606513	0.015616	0.006603	0.002244	0.000094
6.718600E-10	1.996654	2.015504	0.013059	0.005778	0.002007	0.000085
6.936300E-10	1.996678	1.601757	0.011137	0.005264	0.001898	0.000083
7.101700E-10	1.996693	1.278159	0.009606	0.004750	0.001756	0.000078
7.230600E-10	1.996703	1.084867	0.008632	0.004405	0.001658	0.000074
7.304800E-10	1.996713	0.904328	0.007732	0.004010	0.001522	0.000068
7.386500E-10	1.996727	0.655132	0.006416	0.003390	0.001296	0.000059
7.573800E-10	1.996754	0.516038	0.005478	0.003016	0.001178	0.000054
7.681100E-10	1.996777	0.394683	0.004662	0.002621	0.001036	0.000048
7.799100E-10	1.996803	0.300302	0.003950	0.002269	0.000908	0.000043
7.911600E-10	1.996827	0.222494	0.003308	0.001940	0.000784	0.000037
8.031600E-10	1.996848	0.158481	0.002717	0.001629	0.000665	0.000032
8.163500E-10	1.996856	0.112230	0.002228	0.001368	0.000565	0.000027
8.279100E-10	1.996811	0.061314	0.001610	0.001023	0.000426	0.000021
8.477300E-10	1.996645	0.038897	0.001254	0.000832	0.000353	0.000017
8.575400E-10	1.996203	0.023855	0.000970	0.000672	0.000289	0.000014
8.657700E-10	1.994999	0.014036	0.000737	0.000538	0.000236	0.000012
8.734400E-10	1.992706	0.009039	0.000588	0.000453	0.000202	0.000010

Time (s)	<occ1>	<occ2>	<occ3>	<occ4>	<occ5>	<occ6>
8.801600E-10	1.987522	0.005665	0.000465	0.000380	0.000172	0.000009
8.911800E-10	1.982887	0.004605	0.000420	0.000355	0.000163	0.000008
8.993200E-10	1.977705	0.003898	0.000388	0.000335	0.000154	0.000008
9.082000E-10	1.971848	0.003385	0.000363	0.000319	0.000148	0.000007
9.183600E-10	1.966425	0.003057	0.000345	0.000308	0.000143	0.000007
9.279400E-10	1.960348	0.002764	0.000329	0.000296	0.000138	0.000007
9.390000E-10	1.955316	0.002574	0.000317	0.000287	0.000134	0.000007
9.479800E-10	1.949017	0.002363	0.000304	0.000277	0.000129	0.000007
9.596900E-10	1.943569	0.002205	0.000293	0.000268	0.000125	0.000006
9.701800E-10	1.939388	0.002090	0.000284	0.000262	0.000123	0.000006
9.787600E-10	1.934563	0.001974	0.000276	0.000254	0.000119	0.000006
9.892000E-10	1.930604	0.001884	0.000270	0.000248	0.000116	0.000006
9.979500E-10	1.926035	0.001789	0.000263	0.000242	0.000113	0.000006
1.008800E-09	1.922074	0.001704	0.000256	0.000235	0.000110	0.000006
1.018600E-09	1.917894	0.001618	0.000249	0.000228	0.000106	0.000005
1.029700E-09	1.914902	0.001545	0.000243	0.000221	0.000103	0.000005
1.038200E-09	1.911285	0.001474	0.000237	0.000215	0.000100	0.000005
1.049400E-09	1.908450	0.001405	0.000230	0.000208	0.000096	0.000005
1.058900E-09	1.905221	0.001339	0.000223	0.000200	0.000092	0.000005
1.070500E-09	1.901804	0.001260	0.000215	0.000191	0.000088	0.000005
1.084400E-09	1.900191	0.001187	0.000206	0.000182	0.000083	0.000004
1.092000E-09	1.895360	0.001115	0.000198	0.000174	0.000080	0.000004
1.117400E-09	1.892814	0.000983	0.000182	0.000157	0.000071	0.000004
1.136300E-09	1.890763	0.000886	0.000170	0.000144	0.000065	0.000003
1.156400E-09	1.889328	0.000789	0.000157	0.000131	0.000059	0.000003
1.176800E-09	1.888440	0.000694	0.000145	0.000118	0.000053	0.000003
1.197100E-09	1.887890	0.000603	0.000133	0.000106	0.000047	0.000002
1.220700E-09	1.887835	0.000508	0.000120	0.000093	0.000040	0.000002
1.234300E-09	1.887837	0.000453	0.000112	0.000086	0.000037	0.000002
1.265700E-09	1.888071	0.000347	0.000095	0.000071	0.000030	0.000002
1.283700E-09	1.888336	0.000292	0.000086	0.000063	0.000027	0.000001
1.303600E-09	1.888651	0.000239	0.000076	0.000056	0.000024	0.000001
1.325400E-09	1.888996	0.000190	0.000067	0.000048	0.000021	0.000001
1.349300E-09	1.889343	0.000146	0.000057	0.000042	0.000018	0.000001
1.375700E-09	1.889671	0.000108	0.000048	0.000035	0.000015	0.000001
1.404400E-09	1.889966	0.000076	0.000039	0.000030	0.000013	0.000001

Time (s)	<occ1>	<occ2>	<occ3>	<occ4>	<occ5>	<occ6>
1.435600E-09	1.890227	0.000053	0.000032	0.000025	0.000011	0.000001
1.469600E-09	1.890449	0.000036	0.000025	0.000021	0.000010	0.000000
1.506500E-09	1.890646	0.000025	0.000020	0.000018	0.000009	0.000000
1.546500E-09	1.890819	0.000018	0.000017	0.000016	0.000008	0.000000
1.588700E-09	1.891144	0.000014	0.000015	0.000015	0.000007	0.000000
1.678100E-09	1.891465	0.000012	0.000013	0.000014	0.000007	0.000000
1.771000E-09	1.891885	0.000013	0.000014	0.000015	0.000007	0.000000
1.874200E-09	1.892402	0.000015	0.000015	0.000017	0.000008	0.000000
1.974900E-09	1.892914	0.000016	0.000015	0.000016	0.000008	0.000000

Table 2.f. Evolution of germanium plasma fractional orbital populations in the average atom computed with ATMED CR with criteria of convergence in populations of < 5E-04

Time (s)	<occ1>	<occ2>	<occ3>	<occ4>	<occ5>	<occ6>
5.313700E-10	1.996503	6.254325	0.028598	0.005022	0.001271	0.000041
5.539300E-10	1.996490	5.788379	0.028644	0.006458	0.001765	0.000062
5.710200E-10	1.996505	5.004733	0.025228	0.006814	0.001838	0.000067
5.910000E-10	1.996529	4.148696	0.021956	0.006738	0.001930	0.000072
6.100800E-10	1.996564	3.292622	0.018624	0.006307	0.001892	0.000073
6.301000E-10	1.996610	2.393578	0.015022	0.005546	0.001734	0.000069
6.553400E-10	1.996653	1.818179	0.012474	0.005133	0.001703	0.000071
6.718600E-10	1.996685	1.262543	0.009964	0.004302	0.001461	0.000062
6.936300E-10	1.996706	0.906259	0.008111	0.003762	0.001330	0.000058
7.101700E-10	1.996717	0.674243	0.006786	0.003313	0.001204	0.000053
7.230600E-10	1.996723	0.554192	0.006018	0.003052	0.001130	0.000050
7.304800E-10	1.996730	0.444728	0.005308	0.002744	0.001025	0.000046
7.386500E-10	1.996741	0.282491	0.004143	0.002191	0.000826	0.000037
7.573800E-10	1.996765	0.207054	0.003418	0.001889	0.000730	0.000034
7.681100E-10	1.996784	0.145862	0.002797	0.001585	0.000620	0.000029
7.799100E-10	1.996802	0.102275	0.002277	0.001326	0.000526	0.000025
7.911600E-10	1.996809	0.068503	0.001815	0.001086	0.000435	0.000021
8.031600E-10	1.996768	0.042163	0.001384	0.000857	0.000348	0.000017
8.163500E-10	1.996554	0.024968	0.001035	0.000669	0.000276	0.000013
8.279100E-10	1.994789	0.009665	0.000625	0.000438	0.000186	0.000009
8.477300E-10	1.991372	0.006296	0.000494	0.000375	0.000165	0.000008
8.575400E-10	1.987680	0.004946	0.000436	0.000346	0.000154	0.000008
8.657700E-10	1.983917	0.004229	0.000404	0.000330	0.000148	0.000007

8.734400E-10	1.980426	0.003820	0.000385	0.000320	0.000145	0.000007
8.801600E-10	1.974807	0.003303	0.000359	0.000305	0.000139	0.000007
8.911800E-10	1.970364	0.003089	0.000348	0.000301	0.000138	0.000007
8.993200E-10	1.965517	0.002866	0.000337	0.000295	0.000136	0.000007
9.082000E-10	1.959986	0.002653	0.000325	0.000288	0.000133	0.000007
9.183600E-10	1.954759	0.002493	0.000315	0.000282	0.000130	0.000007
9.279400E-10	1.948834	0.002325	0.000305	0.000275	0.000127	0.000006
9.390000E-10	1.944070	0.002212	0.000296	0.000269	0.000125	0.000006
9.479800E-10	1.938086	0.002073	0.000287	0.000262	0.000122	0.000006
9.596900E-10	1.932909	0.001964	0.000278	0.000255	0.000119	0.000006
9.701800E-10	1.928826	0.001879	0.000272	0.000249	0.000116	0.000006
9.787600E-10	1.924076	0.001789	0.000265	0.000243	0.000113	0.000006
9.892000E-10	1.920254	0.001719	0.000259	0.000238	0.000111	0.000006
9.979500E-10	1.915749	0.001642	0.000253	0.000232	0.000108	0.000006
1.008800E-09	1.911916	0.001571	0.000247	0.000226	0.000105	0.000005
1.018600E-09	1.907860	0.001499	0.000241	0.000219	0.000102	0.000005
1.029700E-09	1.904984	0.001436	0.000235	0.000213	0.000098	0.000005
1.038200E-09	1.901430	0.001377	0.000230	0.000208	0.000096	0.000005
1.049400E-09	1.898679	0.001315	0.000223	0.000200	0.000092	0.000005
1.058900E-09	1.895589	0.001255	0.000217	0.000194	0.000089	0.000005
1.070500E-09	1.892283	0.001185	0.000209	0.000186	0.000085	0.000004
1.084400E-09	1.890732	0.001118	0.000200	0.000176	0.000081	0.000004
1.092000E-09	1.886001	0.001054	0.000193	0.000169	0.000077	0.000004
1.117400E-09	1.883500	0.000931	0.000177	0.000152	0.000069	0.000004
1.136300E-09	1.881479	0.000840	0.000165	0.000140	0.000063	0.000003
1.156400E-09	1.880046	0.000749	0.000153	0.000127	0.000057	0.000003
1.176800E-09	1.879142	0.000659	0.000141	0.000115	0.000051	0.000003
1.197100E-09	1.878562	0.000573	0.000129	0.000103	0.000045	0.000002
1.220700E-09	1.878484	0.000482	0.000116	0.000090	0.000039	0.000002
1.234300E-09	1.878414	0.000431	0.000109	0.000083	0.000036	0.000002
1.265700E-09	1.878603	0.000330	0.000093	0.000068	0.000029	0.000001
1.283700E-09	1.878824	0.000277	0.000084	0.000061	0.000025	0.000001
1.303600E-09	1.879091	0.000227	0.000074	0.000053	0.000022	0.000001
1.325400E-09	1.879381	0.000181	0.000065	0.000046	0.000019	0.000001
1.349300E-09	1.879673	0.000138	0.000056	0.000040	0.000016	0.000001
1.375700E-09	1.879944	0.000102	0.000047	0.000034	0.000014	0.000001
1.404400E-09	1.880182	0.000072	0.000038	0.000028	0.000012	0.000001

1.435600E-09	1.880381	0.000049	0.000031	0.000023	0.000010	0.000001
1.469600E-09	1.880541	0.000033	0.000024	0.000019	0.000008	0.000000
1.506500E-09	1.880670	0.000022	0.000019	0.000016	0.000007	0.000000
1.546500E-09	1.880774	0.000014	0.000015	0.000013	0.000006	0.000000
1.588700E-09	1.880945	0.000010	0.000012	0.000011	0.000005	0.000000
1.678100E-09	1.881101	0.000008	0.000010	0.000010	0.000005	0.000000
1.771000E-09	1.881304	0.000008	0.000011	0.000011	0.000005	0.000000
1.874200E-09	1.881556	0.000009	0.000012	0.000012	0.000006	0.000000
1.974900E-09	1.881834	0.000010	0.000012	0.000012	0.000006	0.000000

Table 2.g. Evolution of germanium plasma fractional orbital populations in the average atom computed with ATMED CR with criteria of convergence in populations of < 1.5E-02

Time (s)	<occ1>	<occ2>	<occ3>	<occ4>	<occ5>	<occ6>
4.744100E-10	1.996105	7.927771	5.791694	0.096751	0.016691	0.000274
4.921400E-10	1.996280	7.930947	3.205583	0.063832	0.012852	0.000381
5.101400E-10	1.996436	7.920232	0.323862	0.031224	0.004113	0.000134
5.313700E-10	1.996432	7.591633	0.068911	0.010991	0.003072	0.000100
5.539300E-10	1.996433	6.887844	0.043776	0.009865	0.002828	0.000102
5.710200E-10	1.996446	6.200883	0.035244	0.009405	0.002815	0.000105
5.910000E-10	1.996469	5.416912	0.029559	0.009118	0.002875	0.000110
6.100800E-10	1.996506	4.581123	0.024781	0.008845	0.002772	0.000109
6.301000E-10	1.996552	3.750509	0.020678	0.008057	0.002635	0.000107
6.553400E-10	1.996599	3.106729	0.017655	0.007582	0.002614	0.000110
6.718600E-10	1.996639	2.400766	0.014581	0.006524	0.002291	0.000098
6.936300E-10	1.996667	1.874018	0.012236	0.005817	0.002111	0.000092
7.101700E-10	1.996683	1.534022	0.010665	0.005303	0.001973	0.000087
7.230600E-10	1.996693	1.332982	0.009688	0.004969	0.001883	0.000084
7.304800E-10	1.996703	1.146241	0.008806	0.004589	0.001753	0.000079
7.386500E-10	1.996719	0.876421	0.007497	0.003974	0.001529	0.000069
7.573800E-10	1.996747	0.704217	0.006458	0.003551	0.001398	0.000064
7.681100E-10	1.996770	0.562044	0.005608	0.003153	0.001253	0.000058
7.799100E-10	1.996798	0.448103	0.004859	0.002788	0.001121	0.000053
7.911600E-10	1.996824	0.346531	0.004156	0.002427	0.000986	0.000047
8.031600E-10	1.996848	0.260704	0.003505	0.002087	0.000856	0.000041
8.163500E-10	1.996867	0.196429	0.002964	0.001802	0.000747	0.000036
8.279100E-10	1.996866	0.122333	0.002290	0.001425	0.000595	0.000029
8.477300E-10	1.996839	0.086977	0.001891	0.001212	0.000512	0.000025

Time (s)	<occ1>	<occ2>	<occ3>	<occ4>	<occ5>	<occ6>
8.575400E-10	1.996771	0.061584	0.001575	0.001034	0.000440	0.000022
8.657700E-10	1.996613	0.041628	0.001285	0.000868	0.000373	0.000018
8.734400E-10	1.996253	0.027553	0.001037	0.000726	0.000315	0.000016
8.801600E-10	1.994537	0.013403	0.000716	0.000537	0.000238	0.000012
8.911800E-10	1.991112	0.008070	0.000553	0.000442	0.000200	0.000010
8.993200E-10	1.986190	0.005631	0.000462	0.000387	0.000178	0.000009
9.082000E-10	1.980260	0.004376	0.000409	0.000353	0.000164	0.000008
9.183600E-10	1.974555	0.003716	0.000378	0.000333	0.000155	0.000008
9.279400E-10	1.968070	0.003211	0.000352	0.000315	0.000147	0.000007
9.390000E-10	1.962733	0.002914	0.000335	0.000303	0.000142	0.000007
9.479800E-10	1.956229	0.002621	0.000318	0.000289	0.000136	0.000007
9.596900E-10	1.950426	0.002407	0.000305	0.000278	0.000130	0.000007
9.701800E-10	1.945802	0.002256	0.000295	0.000270	0.000126	0.000007
9.787600E-10	1.940440	0.002106	0.000285	0.000261	0.000122	0.000006
9.892000E-10	1.936106	0.001994	0.000277	0.000254	0.000119	0.000006
9.979500E-10	1.931116	0.001878	0.000269	0.000246	0.000115	0.000006
1.008800E-09	1.926805	0.001779	0.000261	0.000239	0.000111	0.000006
1.018600E-09	1.922274	0.001680	0.000254	0.000231	0.000108	0.000006
1.029700E-09	1.919052	0.001599	0.000247	0.000224	0.000104	0.000005
1.038200E-09	1.915123	0.001519	0.000240	0.000217	0.000101	0.000005
1.049400E-09	1.912075	0.001445	0.000233	0.000210	0.000097	0.000005
1.058900E-09	1.908663	0.001372	0.000226	0.000202	0.000093	0.000005
1.070500E-09	1.905033	0.001289	0.000217	0.000193	0.000089	0.000005
1.084400E-09	1.903338	0.001212	0.000208	0.000184	0.000084	0.000004
1.092000E-09	1.898306	0.001136	0.000200	0.000176	0.000081	0.000004
1.117400E-09	1.895590	0.001000	0.000183	0.000158	0.000072	0.000004
1.136300E-09	1.893426	0.000900	0.000171	0.000145	0.000066	0.000003
1.156400E-09	1.891920	0.000801	0.000158	0.000132	0.000059	0.000003
1.176800E-09	1.891057	0.000703	0.000146	0.000119	0.000054	0.000003
1.197100E-09	1.890550	0.000611	0.000133	0.000107	0.000048	0.000002
1.220700E-09	1.890490	0.000515	0.000120	0.000094	0.000041	0.000002
1.234300E-09	1.890504	0.000460	0.000112	0.000087	0.000038	0.000002
1.265700E-09	1.890745	0.000352	0.000096	0.000072	0.000031	0.000002
1.283700E-09	1.891019	0.000296	0.000086	0.000064	0.000027	0.000001
1.303600E-09	1.891359	0.000242	0.000077	0.000056	0.000024	0.000001
1.325400E-09	1.891717	0.000193	0.000067	0.000049	0.000021	0.000001

Time (s)	<occ1>	<occ2>	<occ3>	<occ4>	<occ5>	<occ6>
1.349300E-09	1.892088	0.000148	0.000057	0.000042	0.000018	0.000001
1.375700E-09	1.892447	0.000109	0.000048	0.000036	0.000016	0.000001
1.404400E-09	1.892775	0.000078	0.000039	0.000031	0.000014	0.000001
1.435600E-09	1.893069	0.000054	0.000032	0.000026	0.000012	0.000001
1.469600E-09	1.893330	0.000037	0.000025	0.000022	0.000011	0.000000
1.506500E-09	1.893569	0.000026	0.000021	0.000019	0.000010	0.000000
1.546500E-09	1.893789	0.000019	0.000017	0.000018	0.000009	0.000000
1.588700E-09	1.894215	0.000016	0.000016	0.000017	0.000008	0.000000
1.678100E-09	1.894633	0.000014	0.000014	0.000016	0.000008	0.000000
1.771000E-09	1.895169	0.000015	0.000015	0.000017	0.000008	0.000000
1.874200E-09	1.895827	0.000018	0.000017	0.000019	0.000009	0.000000
1.974900E-09	1.896542	0.000019	0.000017	0.000019	0.000009	0.000000

Peer-review history:
The peer review history for this paper can be accessed here:
http://www.sdiarticle3.com/review-history/48372